A Platinum Open Access Journal for Organic Chemistry

Review

Free to Authors and Readers | DOAJ Seal | *Arkivoc* **2026** (2) 202612646

Electrochemical properties of Blatter radicals: a survey of cyclic voltammetry data

Georgia A. Zissimou*

Department of Chemistry, University of Cyprus, P.O. Box 20537, 1678 Nicosia, Cyprus
Email: zissimou.georgia@ucy.ac.cy

Received 07-15-2026 **Accepted** 08-19-2026 **Published on line** 09-01-2026

Abstract

Exceptional stability and tunable redox profiles of Blatter radicals are actively driving applications in organic redox-flow batteries, molecular electronics, and spin-based devices. This survey summarizes the electrochemical properties of 1,2,4-benzotriazinyl radicals (Blatter radicals), as determined by cyclic voltammetry. The influence of substitution patterns and structural modifications on redox potentials and electrochemical gaps is discussed, and a brief comparison with other persistent radicals is presented. Electrochemical studies of π-extended, planar, and polyradical Blatter derivatives are not covered.

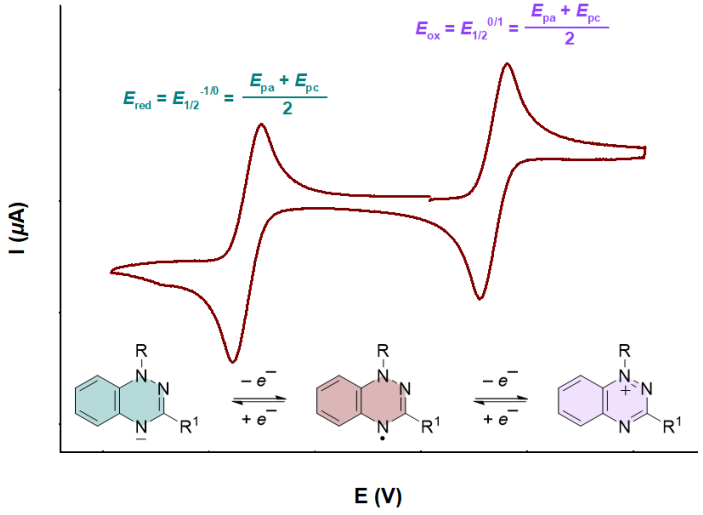

Keywords: 1,2,4-Benzotriazinyl radical, Blatter radical, organic radical, electrochemistry, cyclic voltammetry, redox potential

Table of Contents

1. Introduction
2. Electrochemical Behavior of Blatter Radicals
   2.1. Electrochemical benchmarking of the parent Blatter radical
   2.2. Substituent effects on the redox profile of Blatter radicals
      2.2.1. Substitution at C7
      2.2.2. Substitution at C3
      2.2.3. Substitution at N1
      2.2.4. Substituent effects at electronically-active positions: Additivity and strategic tuning
         2.2.4.1. Regime 1: EWG-dominated systems
         2.2.4.2. Regime 2: Donor–acceptor systems
         2.2.4.3. Additivity and design implications
      2.2.5. Substituent effects with limited electronic coupling
         2.2.5.1. Inductive-dominated modulation (C5, C6)
         2.2.5.2. Through-space interactions in axial systems
         2.2.5.3. Electronic insulation of bulky groups
         2.2.5.4. Design implications
3. Solvent and Electrolyte Effects on Redox Behavior of Blatter Radicals
4. Brief Comparison with Other Persistent Organic Radical Families
5. Conclusions

Acknowledgements
Supplementary Material
References

1. Introduction

1,2,4-Benzotriazinyl radicals (commonly known as Blatter radicals), first reported by Blatter and Lukaszewski in 1968,[1] and shortly after by Huisgen and Wulff,[2] represent an important class of persistent heteroaromatic radicals displaying remarkable stability (for up to 30 years).[3] This stability arises from extensive delocalization of the unpaired electron across the triazinyl ring and fused-benzene framework (Scheme 1), enabling isolation and handling under ambient conditions.

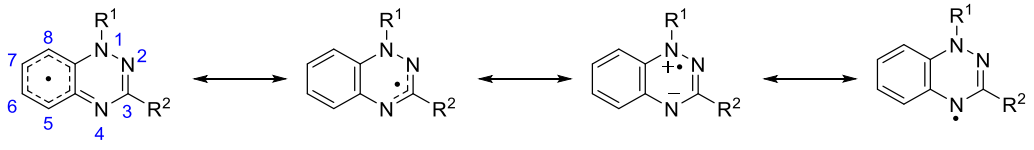

Scheme 1. Delocalization of the unpaired electron in Blatter radicals. IUPAC numbering in blue.

In the 1980s, detailed spectroscopic and electronic structure studies of these radicals were reported by Neugebauer,[4–6] as well as by Kadirov.[7] This early work was followed by sporadic investigations through the 1990s

and early 2000s addressing magnetic properties,[8] charge-transfer (CT) salts,[9] crystal structures,[3,10] and electron-spin resonance (ESR).[11]

Renewed interest emerged approximately a decade later, driven by a pivotal advance in synthetic methodology reported by Koutentis and Lo Re. By identifying amidrazone purity as the critical determinant of radical yield, they established a robust and reproducible route based on Pd/C/DBU-mediated aerobic oxidation.[12] This catalytic protocol replaced earlier stoichiometric oxidative methods employing HgO, Ag_2O or $K_3[Fe(CN)_6]$ with a cleaner, safer, and operationally simple approach, effectively removing a major bottleneck in the preparation of Blatter radicals. As a result, access to these systems became routine and enabled their broader exploration.

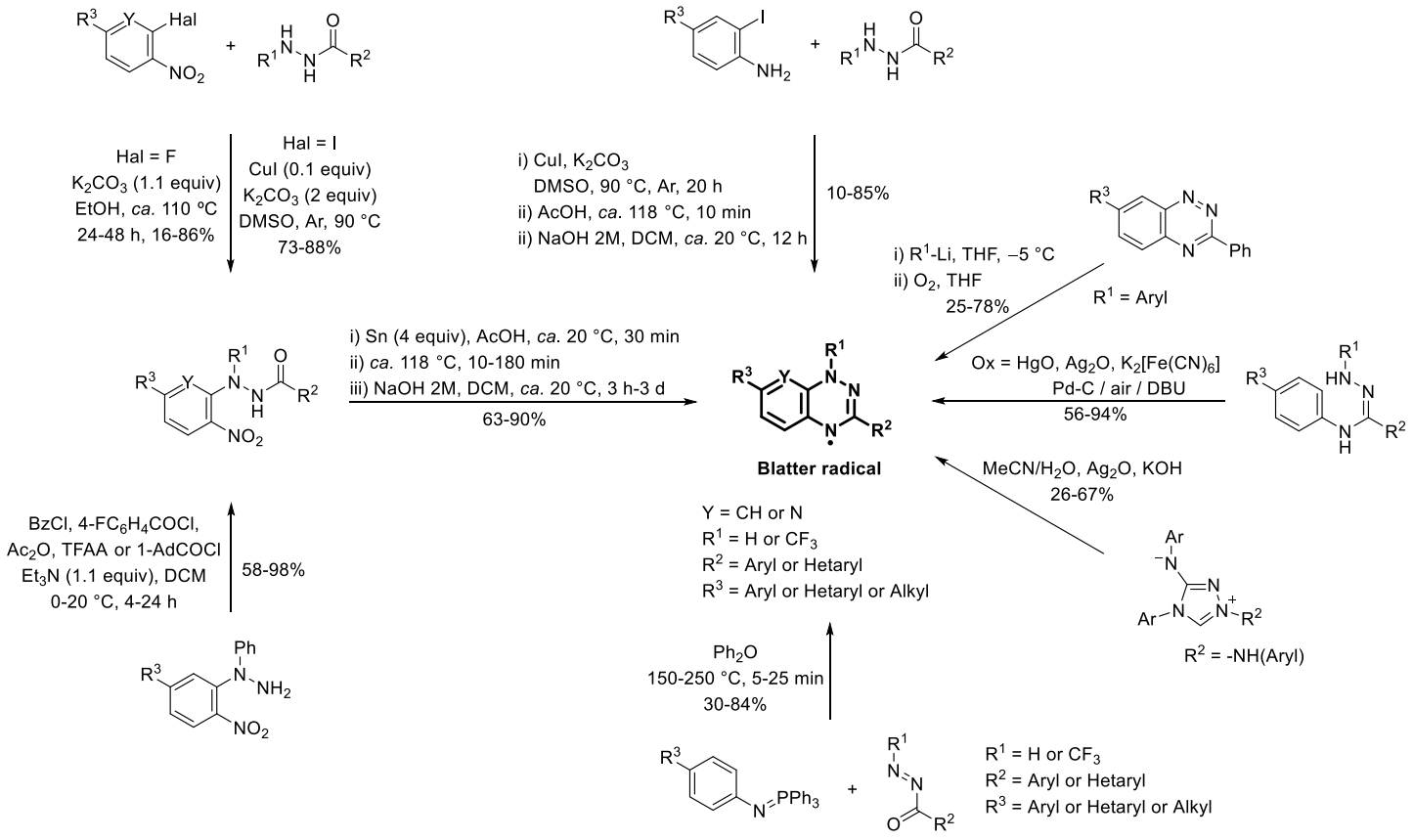

Scheme 2. Blatter radical synthetic methods.

The following decade saw a rapid expansion of synthetic strategies (Scheme 2). Further methodological development by Koutentis and co-workers established multiple synthetic entries to the Blatter radical framework,[13–15] that systematically expanded its structural diversity. These included the preparation of *N*′-(het)aryl-*N*′-[2-nitro(het)aryl]hydrazides by two synthetic methods, followed by reduction of the nitro group to the corresponding aminohydrazides, acid-mediated cyclodehydration to the corresponding benzotriazines, and base-mediated oxidation to the radicals; a complementary CuI-mediated C-N coupling of iodoaniline with appropriate *N*-(het)aryl-(het)arylhydrazides to generate the corresponding aminohydrazides, followed again by cyclodehydration to the benzotriazine framework and base-mediated oxidation to the radicals; and an aza-Wittig approach in which *N*-aryliminophosphoranes reacted with 1-(het)aroyl-2-aryldiazenes to furnish Blatter radicals directly. Significant and complementary advances were subsequently achieved by Kaszyński[16,17] and

O'Donoghue.[18] Kaszyński's approach involved addition of an aryllithium reagent to a prepared benzotriazine followed by aerial oxidation, whereas O'Donoghue's method introduced a cascade reaction involving hydrolytic ring opening of Nitron, followed by oxidative cyclization to afford C3-amido-substituted Blatter radicals. Across these efforts, functional group transformations[19] and C–C coupling methodologies[20,21] demonstrated that extensive derivatization could be achieved without compromising radical stability.

Treatment of these radicals with mild reducing agents, such as ascorbic acid[19] or phenylhydrazine,[4] resulted in the *leuco* triazine, while mild oxidizing agents, such as silver nitrate ($AgNO_3$) and ferric chloride ($FeCl_3$), gave mainly benzotriazinium salts,[4] allowing characterization by nuclear magnetic resonance (NMR) (Scheme 3). Tetranitromethane ($C(NO_2)_4$) was also reported to oxidize the radical to the corresponding benzotriazinium salt, which was trapped as the perchlorate salt with perchloric acid ($HClO_4$). Interestingly, these redox processes were reversible, and the radical could be regenerated upon treatment with sodium periodate[19] ($NaIO_4$) or a base, *e.g.*, triethylamine,[4] respectively. In contrast, treatment with Zn in refluxing AcOH led to ring-contracted imidazoles,[22] whereas treatment with strong oxidants, such as manganese dioxide (MnO_2), gave 1,2,4-benzotriazin-7-ones[2,4,12,13,23] (Scheme 3).

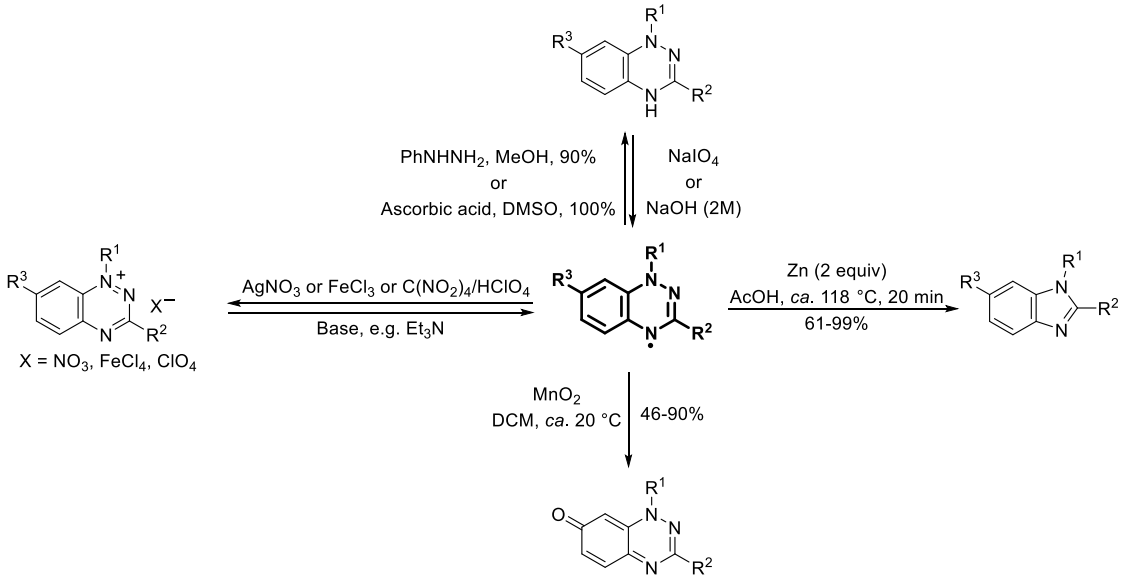

Scheme 3. Redox chemistry of Blatter radicals.

The benzotriazinone, despite being a product derived from oxidative degradation of the neutral radical, is a useful precursor to new azolo-fused Blatter radicals. Nucleophilic functionalization at C6 provided benzotriazin-6-yl carboxamides or benzimidamides, which upon heating with phosphorus pentasulfide (P_2S_5) or in acetic acid underwent cyclization to afford thiazolo-[24] and imidazolo-[25] fused radicals, respectively (Scheme 4). An oxazolo-fused[25] radical was also isolated as a side product.

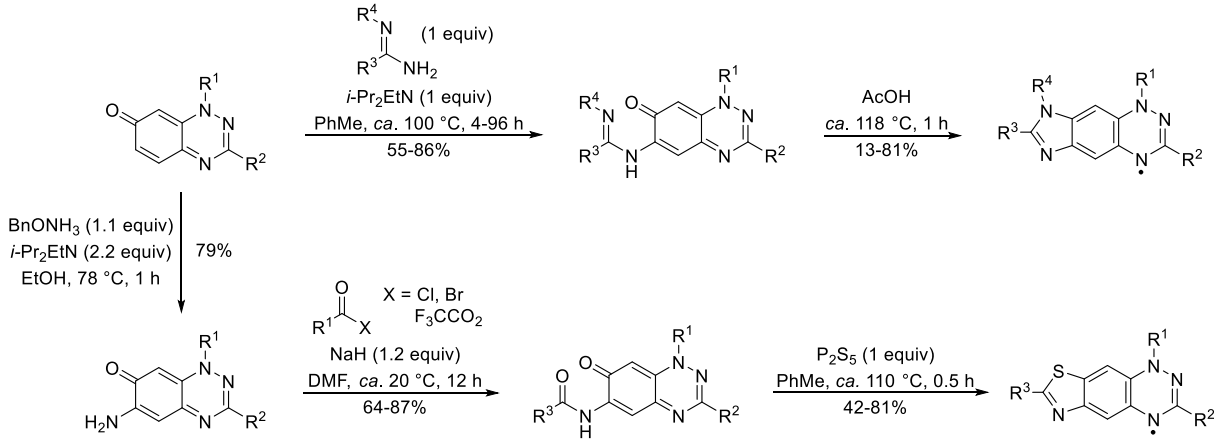

Scheme 4. Selective chemistry of 1,2,4-benzotriazin-7-one.

Metal-coordinated radicals[26–32] and liquid crystalline materials with discotic[33–35] and photoconductive bent-core structures[36–38] were reported, along with a new class of sulfur-[39] and oxo-[40–47] fused-planar Blatter radicals. Interest has also been directed toward higher-spin architectures including diradicals,[48–51] triradicals[52–55] and tetraradicals.[56]

Although typically non-emissive, selected Blatter radicals have shown weak white-light emission,[57] while suitably engineered thiol-functionalized derivatives can display measurable photoluminescence under plasmonic conditions.[58] For Blatter radicals, antiferromagnetic interactions are commonly observed in π-stacked systems,[59–64] whereas ferromagnetic coupling has been reported in appropriately designed or structurally favorable systems,[64–70] while other analogues exhibit spin-transition behavior,[14,71,72] highlighting the sensitivity of magnetic coupling to subtle structural variations. Computational studies provide insight into spin distribution and exchange mechanisms,[73,74] while surface-supported and sterically hindered systems highlight cases of paramagnetic behavior with minimal intermolecular coupling.[75,76]

Blatter radicals have been studied in a variety of applications. In the realm of chemical synthesis, they serve as mediators in styrene polymerization,[77,78] function as polymerization radical initiators,[79,80] and can act as picric acid sensors.[81] They are stable enough to be integrated into metal–organic frameworks (MOFs) as radical linkers.[82] Their unique electronic profile has seen them gain interest as redox-active blocks in organic batteries[83–86] and their persistent spin and favorable spin transport make them promising components for organic spintronic devices,[87,88] and molecular memristors,[89] as well as potent dynamic nuclear polarization agents.[90–92]

Despite extensive studies on the structure and reactivity of Blatter radicals, as well as recent reviews,[93–96] a systematic understanding of their electrochemical properties remains fragmented. This review focuses on the electrochemical behavior of Blatter radicals up to early 2026, highlighting how substitution patterns and structural modifications influence their redox potentials and electrochemical gaps. Electrochemical studies of fused "π-extended", planar, and polyradical Blatter systems fall outside the scope of this review and will not be discussed.

2. Electrochemical Behavior of Blatter Radicals

Blatter radicals commonly exhibit bipolar electrochemistry, undergoing one reversible oxidation and one reversible reduction corresponding to the cationic and anionic states, respectively (Scheme 5). This reversibility

demonstrates the intrinsic stability on the electrochemical timescale of all accessible redox states and underpins their suitability for applications such as organic redox-flow batteries[84] and spintronic devices.[87,88]

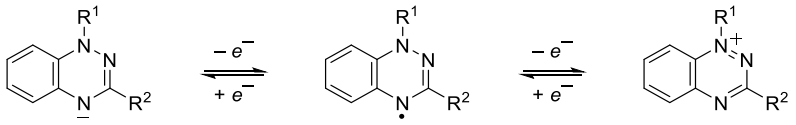

Scheme 5. Redox processes of Blatter radicals.

In cyclic voltammetry (CV), this behavior manifests as two well-defined and typically reversible waves (Figure 1). Reversibility is assessed by the peak-to-peak separation ($\Delta Ep = |Epa - Epc|$) and the anodic-to-cathodic peak current ratio ($i_p = i_{pa} / i_{pc}$). For an ideal one-electron process, $\Delta Ep \approx 59$ mV and $i_p \approx 1$; Blatter radicals generally approach these values, with reported ΔEp in the range of ~63–74 mV[90,97] and i_p close to unity.

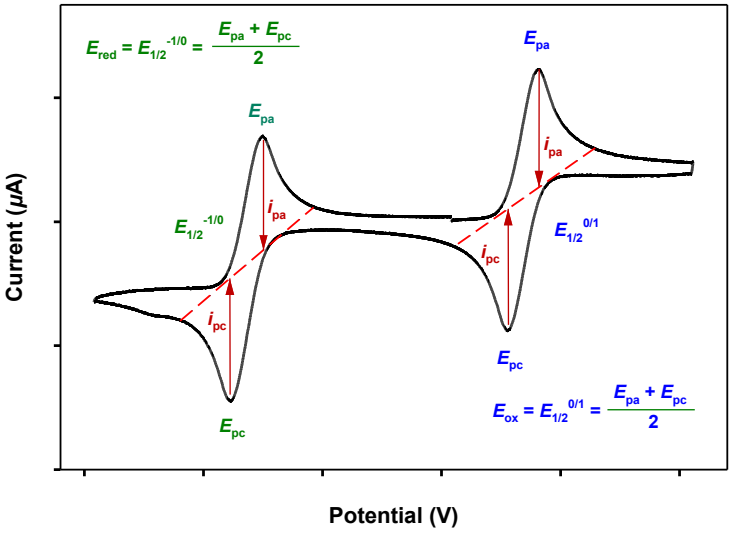

Figure 1. Typical Blatter radical CV showing Ep, i_p and $E_{1/2}$ for each redox process.

Electrochemical measurements are performed using CV, often complemented by differential pulse voltammetry (DPV), typically using degassed solutions under an inert atmosphere (N_2 or Ar). Experiments are generally conducted in anhydrous organic solvents, most commonly dichloromethane (DCM), but also acetonitrile (MeCN) and dimethylformamide (DMF), in the presence of a tetrabutylammonium supporting electrolyte, *e.g.*, *n*-Bu_4NPF_6 or, in earlier studies, *n*-Bu_4NBF_4. Standard three-electrode configurations are employed, typically comprising a glassy carbon or Pt working electrode, a platinum counter electrode, and an Ag/AgCl-based reference electrode.

To enable consistent comparison across studies, redox potentials are referenced to the ferrocene/ferrocenium (Fc/Fc^+) couple ($E_{Fc/Fc^+} = 0.0$ V), either measured directly or converted from other reference electrodes such as Ag/AgCl or saturated calomel electrode (SCE). These conversions depend on the electrochemical set up, including electrodes and electrolyte. While the working (Pt or glassy C) and counter (usually Pt) electrodes are broadly similar across studies, electrode material and surface properties can influence electrochemical responses. However, no systematic working and counter electrode-dependent trends could be

identified within the datasets compiled in this review. The choice of reference electrode, however, varies considerably between studies: Pt wire and a variety of Ag/Ag^+ pseudo electrodes have been employed as the reference electrodes, with Fc/Fc^+ as the internal standard. In nonaqueous media, the use of such external reference electrodes, aqueous SCE or Ag/Ag^+ pseudo-references introduces significant and often unstable liquid junction potentials, which affect the measured redox processes and shift the potentials. Potential stability and reproducibility of these electrodes are often additional issues to be considered. In an early study by Gagné, Koval and Lisensky,[98] it was demonstrated that the redox potential of the Fc/Fc^+ couple remains constant relative to an analyte within a given solvent, effectively making the measured potential independent of the choice of reference electrode; thus the Fc/Fc^+ couple has found widespread use as internal reference. The electrolyte (e.g., *n*-Bu_4NBF_4) concentration though, affects the Fc/Fc^+ redox potential, as the alteration of the dielectric constant and ion-pairing environment in DCM, MeCN and DMF changes.[99] While the half-wave potential of Fc/Fc^+ (E_{Fc/Fc^+}) in MeCN and DMF shifts ~30 mV in electrolyte concentrations between 50 and 500 mM, the difference in DCM is around 100 mV, affecting even measurements with the same electrolyte when its concentration changes. Consequently, the variation in reported potentials is a function of both the reference electrode and the electrolyte-dependent stabilization of the redox couples, and authors should take these factors into consideration when comparing electrochemical data. In most articles, the Fc/Fc^+ is typically set to 0.460 V in MeCN and 0.475 V in DCM solutions of *n*-Bu_4NPF_6 (0.1 M) *vs* SCE and 0.400 V in MeCN and 0.352 V in DCM solutions of *n*-Bu_4NBF_4 (0.1 M) systems *vs* SCE and Ag/AgCl, respectively, illustrating the electrolyte and reference solvent variation.[98–103] We should note here that, in several Blatter radical articles, the redox values are discussed against the Fc/Fc^+ couple in the main text, however, the authors report $E_{Fc/Fc^+} \neq 0$ V. Where these discrepancies occur, the adjustment versus the Fc/Fc^+ couple will be made according to the E_{Fc/Fc^+} value reported in the article, irrespective of the electrochemical cell conditions. In the following section, the electrochemical behavior of the parent Blatter radical, 1,3-diphenyl-1,4-dihydrobenzo[*e*][1,2,4]triazin-4-yl,[1] is used as a reference point for comparison, and these effects are discussed in more detail.

2.1. Electrochemical benchmarking of the parent Blatter radical

The electrochemical behavior of the parent Blatter radical has been extensively investigated by CV and DPV under a range of conditions (Table 1). The very first report of the radical's CV, by Hutchison *et al.*,[9] was measured in MeCN with *n*-Bu_4NBF_4 (0.1 M) as electrolyte and $Ag/AgNO_3$ (nonaqueous) as the reference electrode, utilizing Fc/Fc^+ as internal reference (Table 1, entry 1). The half-wave potentials $E_{1/2}{}^{-1/0} = -0.960$ V and $E_{1/2}{}^{0/+1} = 0.103$ V were reported against SCE, *i.e.*, $E_{1/2}{}^{-1/0} = -1.36$ V and $E_{1/2}{}^{0/+1} = -0.30$ V vs Fc/Fc^+, respectively. Several subsequent comparisons with other analogues, even if referenced against other electrodes such as Ag/Ag^+, have been made using the original exact redox values. Thus, the relevant sections should be discussed with caution, as the original redox values were retained without applying the corresponding corrections for the different electrochemical conditions.

In a more recent measurement in MeCN (Table 1, entry 2), the redox potentials are reported ~0.1 V more positive, a possible effect of the employed electrolyte (*n*-Bu_4NPF_6) while the ΔE_{cell} remains ~1.0 V. This suggests weak specific-ion pairing and weak electrolyte interactions under these conditions.[104–107] However, this conclusion is based on only two datasets, and the observed spread reflects inter-laboratory variability, including differences in reference-electrode calibration, electrolyte identity, and experimental conditions, rather than a single intrinsic uncertainty.

Protic media substantially perturb the redox behavior by selectively stabilizing the anion through hydrogen bonding and increased dielectric stabilization. Steen and co-workers systematically incorporated water into

MeCN (up to 33% v/v) and observed a significant anodic shift of the reduction potential, while the oxidation remained comparatively insensitive (*cf.* entries 2 vs 3). This response led to a marked compression of ΔE_{cell} (entry 3, 0.50 V), consistent with preferential stabilization.[84]

In DCM (Table 1, entries 4–6), reported reduction potentials span from −1.38 to −1.32 V, while oxidation potentials are reported at −0.17 to −0.18 V, giving electrochemical gaps from 1.15 to 1.20 V. Interestingly, in the measurement where the reduction potential appears at −1.38 V (entry 5), the electrolyte concentration is only half (50 mM) of the most common 100 mM, which, as seen, affects the solvent's dielectric constant. Across the DCM datasets, the electrolyte identity is unchanged, although its concentration varies.

Overall, within the DCM/*n*-Bu_4NPF_6 subset (entries 4–6), the corresponding mean values are $E_{1/2}^{-1/0} \approx -1.34 \pm 0.03$ V and $E_{1/2}^{0/+1} \approx -0.17 \pm 0.01$ V, with $\Delta E_{cell} \approx 1.17 \pm 0.03$ V, indicating that, under a fixed solvent–electrolyte framework, ΔE_{cell} is relatively well conserved. Notably, two independent measurements converge in a narrow range of 1.15–1.16 V. Accordingly, $\Delta E_{cell} \approx 1.15$–1.16 V is adopted as a practical benchmark for comparison across structurally-modified derivatives, while the aprotic solvent range (1.04–1.20 V) is retained as the experimental envelope.

Table 1. Summary of the electrochemical redox potentials of the parent Blatter radical as measured by CV at *ca*. 20 °C with a scan rate of 50 or 100 $mV \cdot s^{-1}$. The redox potentials are stated as reported in the literature and referenced vs Fc/Fc^+ ($E_{Fc/Fc^+} = 0.0$ V)

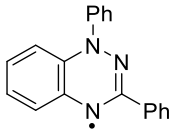

The parent Blatter radical

			Reported			*Referenced vs Fc/Fc⁺*			
Entry	Solvent	Electrolyte	$E_{1/2}^{-1/0}$ (V)	$E_{1/2}^{0/+1}$ (V)	ΔE_{cell} (V)	$E_{1/2}^{-1/0}$ (V)	$E_{1/2}^{0/+1}$ (V)	ΔE_{cell} (V)	Ref.
1	MeCN[a]	*n*-Bu_4NBF_4	−0.960	+0.103	1.063	−1.36	−0.30	1.06	9
2	MeCN[b]	*n*-Bu_4NPF_6	−1.24	−0.20	1.04	−1.24	−0.20	1.04	84
3	MeCN/H_2O[c] 2/1 (v/v)	*n*-Bu_4NPF_6	−0.71	−0.21	0.50	−0.71	−0.21	0.50	84
4	DCM[d]	*n*-Bu_4NPF_6	−0.864	+0.288	1.152	−1.32	−0.17	1.15	15
5	DCM[e]	*n*-Bu_4NPF_6	−0.92	+0.28	1.20	−1.38	−0.18	1.20	16
6	DCM[f]	*n*-Bu_4NPF_6	−0.853	+0.310	1.163	−1.33	−0.17	1.16	52

[a] E_{Fc/Fc^+} = 0.40 V vs SCE, 0.1 M electrolyte, Pt disk (working), $Ag/AgNO_3$ (nonaqueous); [b] Referenced vs Fc/Fc^+, Pt wire (counter), glassy C (working), Ag/Ag^+ (0.01 M $AgPF_6$ in 0.1 M Bu_4NPF_6) single junction (reference); [c] Referenced vs Fc/Fc^+, Pt wire (counter), glassy C (working), SCE (reference); [d] E_{Fc/Fc^+} = 0.46 V vs SCE, 0.1 M electrolyte, Pt wire (counter), glassy C (working), Ag/AgCl (1 M KCl) (reference); [e] E_{Fc/Fc^+} = 0.46 V vs SCE, 50 mM electrolyte, Pt wire (counter), glassy C (working), Ag/AgCl (reference); [f] E_{Fc/Fc^+} = 0.475 V vs SCE, 0.1 M electrolyte, Pt wire (counter), glassy C (working), Ag/AgCl (reference).

2.2. Substituent effects on the redox profile of Blatter radicals

Substitution at the C7, C3, and N1 positions (Figure 2) provides a systematic means of tuning the redox properties of Blatter radicals, influencing both oxidation and reduction processes in distinct and predictable ways. These effects arise from a balance of inductive and resonance contributions, which depend strongly on the substitution site.

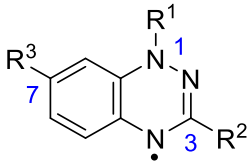

Figure 2. Typical substitution patterns for Blatter radicals at positions C7, C3 and N1.

2.2.1. Substitution at C7. Electron-withdrawing groups (EWGs) at C7, such as CF_3 and CN (Table 2, entries 4–6), shift both redox processes to more anodic potentials. For example, $E_{1/2}^{-1/0}$ shifts from *ca.* −1.32 V in the parent radical (entry 1) to between −1.16 and −1.19 V for CF_3 derivatives (entries 5 and 6) and to −1.09 V for the CN derivative (entry 4), reflecting stabilization of the anionic state. Correspondingly, $E_{1/2}^{0/+1}$ shifts anodically from −0.17 V (parent) to +0.02 V (CF_3) and +0.08 V (CN), indicating that electron withdrawal lowers the energy of the neutral radical and increases the potential required for oxidation.

Conversely, the C7–Me substituent (entry 20) shifts both redox processes to more cathodic values: $E_{1/2}^{-1/0}$ moves to −1.40 V, and $E_{1/2}^{0/+1}$ to −0.27 V. This behavior is consistent with increased electron density at the radical center and can be attributed to hyper-conjugative σ(C–H)→ singly-occupied molecular-orbital (SOMO) donation from the alkyl substituent.

Halogens (entries 7–11) show intermediate behavior. Fluorine (entry 7) is nearly indistinguishable from the parent in both reduction (−1.31 V) and oxidation (−0.18 V), consistent with partial compensation between inductive withdrawal and weak π-donation. For Cl, Br, and I, poor orbital overlap renders π-donation negligible; inductive effects dominate, leading to modest anodic shifts in both reduction (+0.06 to +0.09 V) and oxidation (+0.07 to +0.09 V).

π-Extended-C7-(het)aryl substituents (entries 12–18) induce only minor perturbations, consistent with limited electronic communication with the radical core despite the extended π-framework. This behavior may reflect modest spin communication with the substituent and/or compensation between inductive and resonance effects. In contrast, the highly conjugated C(Ph)=CPh_2 substituent (entry 19) predominantly influences the oxidation process, leading to a modest increase in the electrochemical gap (ΔE_{cell} ≈ 1.23 V). Notably, the reported cyclic voltammogram differs from the characteristic electrochemical response of Blatter radicals. While both redox processes appear reversible, the oxidation and reduction waves are markedly unequal in magnitude, complicating comparison with the remainder of the series. Accordingly, conclusions regarding the electronic influence of the C(Ph)=CPh_2 substituent should be regarded as tentative.

Overall, substitution at C7 produces relatively small changes in ΔE_{cell} (≈ 1.03–1.23 V). This reflects a combination of modest electronic coupling to the radical core and compensating, state-specific stabilization effects, such that changes in the individual redox potentials partially offset one another.

2.2.2. Substitution at C3. Substituents at C3 (Table 2, entries 21–54) exert a stronger influence on redox properties than those at C7. In DCM the reduction potentials range from −1.49 (*t*-Bu, entry 38) to −1.12 V (CF_3,

entry 22) and oxidation potentials from −0.45 (pyrrolidin-1-yl, entry 47) to +0.13 V (CF_3, entry 22), yielding electrochemical gaps of ΔE_{cell} ≈ 1.01–1.32 V. EWGs, such as CF_3 (entries 21–23) shift both redox processes anodically, while electron-donating groups (EDGs), particularly alkyl (entries 37–43) and amino (entries 44–48) substituents, shift them cathodically.

Absolute potentials are sensitive to the electrochemical medium. For example, the *t*-Bu derivative exhibits a 200 mV anodic shift when moving from DCM (entry 38, $E_{1/2}^{-1/0}$ = −1.49 V) to MeCN (entry 39, $E_{1/2}^{-1/0}$ = −1.29 V). Aniline and amide derivatives (entries 49–54) similarly show higher oxidation potentials in MeCN, reflecting the more polar solvent environment. The amide-substituted derivatives also present smaller electrochemical gaps (ΔE_{cell} ≈ 0.89–0.98 V).

Mechanistically, the pronounced C3 effect arises from its location near a node in the SOMO of the neutral radical and the highest occupied molecular orbital (HOMO) of the reduced (anionic) species (Figure 3).

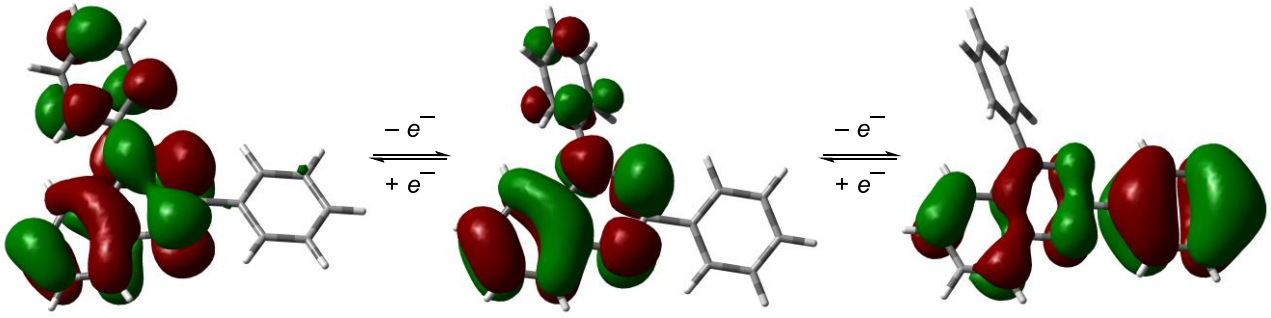

Figure 3. HOMO/SOMO molecular orbital plots of the Blatter radical in its anionic (left), radical (center), and cationic (right) states in the gas phase. Isovalue = 0.02.

This nodal character limits π-delocalization to-and-from the C3 substituent in the neutral and reduced states, making reduction potentials largely governed by inductive (field) effects. In the oxidized (cationic) form, the nodal restriction is alleviated, allowing effective conjugation with the substituent; consequently, oxidation potentials reflect a combination of inductive and resonance contributions. This state-dependent electronic response is supported by Swain–Lupton and Hammett-type analyses, which show dominant field effects in reduction and mixed field/resonance contributions in oxidation.[17,96] Calculations to obtain the HOMO/SOMO molecular orbital plots shown in Figure 3 were performed as part of the present review to support the mechanistic interpretation. The computational methodology and Cartesian coordinates are provided in the Supplementary Material.

A computational approach to redox potentials has been demonstrated for selected C3-substituted Blatter radicals. Pomikło *et al*. compared experimental oxidation potentials with Hammett σ_p parameters for a series of C3-functionalized derivatives,[17] while a subsequent study[108] found good correlations of both redox processes with the pK_a values of the corresponding amines. In the latter study, the oxidation process was also modelled using a DCM dielectric medium, demonstrating a strong correlation between calculated and experimental oxidation potentials for this substitution series.

2.2.3. Substitution at N1. N1 substituents (entries 55–64) produce modest and mostly consistent shifts in both redox potentials, with reduction potentials spanning −1.47 to −1.08 V and oxidation potentials from −0.22 to +0.11 V, yielding ΔE_{cell} ≈ 1.00–1.32 V. Electron-withdrawing (het)aryl groups (entries 55–62) shift the redox

potentials anodically; for example, the C_6F_5 derivative (entry 55) exhibits $E_{1/2}^{-1/0}$ = −1.22 V and $E_{1/2}^{0/+1}$ = +0.11 V, corresponding to shifts of +0.10 and +0.28 V, respectively, relative to the parent Blatter radical (entry 1). In contrast, the electron-donating 2-methoxyphenyl substituent (entry 63) predominantly shifts the reduction potential cathodically ($E_{1/2}^{-1/0}$ = −1.47 V), with a smaller effect on oxidation ($E_{1/2}^{0/+1}$ = −0.22 V) shifted by −0.15 and −0.05 V relative to the parent Blatter radical (entry 1).

While some N1 substituents produce slightly larger shifts in individual redox potentials, the resulting variation in ΔE_{cell} remains moderate (≈ 1.00–1.32 V). Overall, ΔE_{cell} is relatively insensitive to N1 substitution, reflecting limited net electronic communication with the triazinyl radical, likely due to a large dihedral angle between the N1 substituent and the radical core that restricts π-conjugation. It should be noted that for entries 56–59 the potentials were reported versus an Ag/AgCl reference electrode without internal ferrocene (or similar) calibration[109]; consequently, these values should be interpreted with caution.

2.2.4. Substituent effects at electronically-active positions: Additivity and strategic tuning.

The effects of substituents at C3, C7, and N1, discussed in the preceding sections, combine in multi-substituted derivatives to enable systematic modulation of both half-wave potentials and ΔE_{cell}. Across the systems summarized in Table 2, these cumulative effects define two recurring patterns of behavior based on substituent combinations and their impact on ΔE_{cell}. The following analysis emphasizes qualitative trends; absolute values should be interpreted in light of experimental variability. For consistency, only data collected in DCM are considered, as solvent significantly influences reduction potentials.

2.2.4.1. *Regime 1: EWG-dominated systems.* Radicals with multiple strong EWGs generally show larger anodic shifts in both redox potentials compared with the parent Blatter radical or derivatives hosting only one EWG, consistent with roughly additive substituent effects. For example, the 3,7-bis-CF_3 radical (entry 66) exhibits $E_{1/2}^{-1/0}$ = −0.93 V and $E_{1/2}^{0/+1}$ = +0.31 V in DCM, corresponding to shifts of +0.39 and +0.48 V, respectively, relative to the parent (entry 1), while the C3-mono-CF_3 derivative (entry 23) shifts by only +0.08 and +0.07 V. Similarly, the N1-C_6F_5/C3-CF_3 radical (entry 79) exhibits $E_{1/2}^{-1/0}$ = −0.98 V and $E_{1/2}^{0/+1}$ = +0.34 V in DCM, corresponding to shifts of +0.34 and +0.51 V, while the N1-mono-C_6F_5 derivative (entry 55) shifts by +0.10 and +0.28 V. Despite these substantial anodic shifts, the overall redox window (ΔE_{cell}) changes only modestly, indicating that the range between reduction and oxidation potentials remains largely preserved.

2.2.4.2. *Regime 2: Donor–acceptor systems.* Donor–acceptor radicals, in which EDG and EWG groups are combined at electronically coupled positions, exhibit partial cancellation of substituent effects. This typically results in compression of the overall redox window (ΔE_{cell}) relative to EWG-dominated systems. Representative examples include entry 67 (C3-*t*-Bu/C7-CF_3), with $E_{1/2}^{-1/0}$ = −1.11 V, $E_{1/2}^{0/+1}$ = −0.04 V, ΔE_{cell} = 1.07 V; entry 76 (C3-thien-2-yl/C7-CF_3), $E_{1/2}^{-1/0}$ = −1.14 V, $E_{1/2}^{0/+1}$ = +0.03 V, ΔE_{cell} = 1.17 V; and entry 82 (C3-thien-2-yl/N1-4-NCC_6H_4), $E_{1/2}^{-1/0}$ = −1.02 V, $E_{1/2}^{0/+1}$ = −0.02 V, ΔE_{cell} = 1.00 V. In these cases, the donor substituent facilitates oxidation, while reduction remains dominated by the acceptor, producing compressed electrochemical gaps.

2.2.4.3. *Additivity and design implications.* Across these regimes, substituent effects are most clearly additive in the individual redox potentials, while ΔE_{cell} is less sensitive and typically varies within a narrower range (~0.1–0.3 V) within each regime. Consequently, tuning strategies primarily shift the redox window rather than substantially expanding it.

2.2.5. Substituent effects with limited electronic coupling. In contrast to the additive behavior observed in multi-substituted systems (Section 2.2.4), certain positions exhibit limited electronic communication with the

radical core. These electronically weakly coupled positions (Figure 4) allow introduction of specific physical properties or structural constraints without significantly altering the Blatter radical's redox profile.

2.2.5.1. *Inductive-dominated modulation (C5, C6).* Positions C5 and C6 have low spin density, limiting π-conjugative interactions with the radical center. Consequently, substituents at these sites influence redox behavior predominantly through inductive effects. CF_3 substituents at C5 and C6 result in reduction potentials ($E_{1/2}^{-1/0} \approx -1.25$ V)[92] comparable to mono-substituted C3 or C7 analogues, but more cathodic than the cumulative shift seen in C3,C7-bis-CF_3 derivatives. Oxidation potentials ($E_{1/2}^{0/+1} \approx -0.04$ to 0.03 V) remain close to C7-CF_3 values. A 6,7-dicyano-substituted Blatter radical illustrates this behavior: despite pronounced anodic shifts in both redox processes ($E_{1/2}^{-1/0} = -0.96$ V; $E_{1/2}^{0/+1} = 0.25$ V), its overall electrochemical behavior remains consistent with that of simpler analogues.[110]

2.2.5.2. *Through-space interactions in axial systems.* Axially substituted (atropisomeric) Blatter radicals restrict electronic communication by geometry. These systems show reduction potentials from −1.13 to −1.08 V and oxidation potentials from 0.15 to 0.23 V, with relatively large ΔE_{cell} (≈ 1.24–1.34 V). Limited rotation about the C–C bond restricts conjugation, so observed anodic shifts potentially arise from intramolecular π–π interactions rather than resonance, representing a distinct mode of electronic modulation.[111]

2.2.5.3. *Electronic insulation of bulky groups.* Bulky substituents, such as the 3,4,5-tridodecyloxyphenyl groups, illustrate steric electronic insulation. When installed at C3 and C6, oxidation potentials shift marginally (~0.07 V), and reduction potentials (−0.87 to −1.14 V) remain largely dependent on the N1 substituent. These groups allow tuning of solubility, phase behavior or molecular geometry without affecting core electrochemical properties.[33,34]

2.2.5.4. *Design implications.* Positions C5, C6, and sterically hindered axial sites often act as "spectator groups" enabling decoupling of physical property optimization from redox performance. Understanding these electronically isolated positions provides precise control over Blatter radical design and sets the stage for analyzing fused systems, where π-extension and planarity determine whether a substituent fundamentally alters the radical core or remains electronically decoupled.

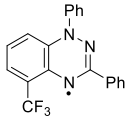

$E_{1/2}^{-1/0}$ (V)	$E_{1/2}^{0/+1}$ (V)	E_{cell} (V)
–1.248	–0.025	1.223

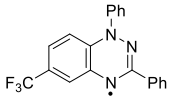

$E_{1/2}^{-1/0}$ (V)	$E_{1/2}^{0/+1}$ (V)	E_{cell} (V)
–1.248	0.035	1.283

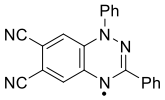

$E_{1/2}^{-1/0}$ (V)	$E_{1/2}^{0/+1}$ (V)	E_{cell} (V)
–0.963	0.245	1.208

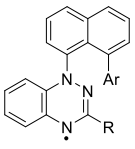

R	Ar	$E_{1/2}^{-1/0}$ (V)	$E_{1/2}^{0/+1}$ (V)	E_{cell} (V)
Ph	Ph	–1.08	0.23	1.31
Ph	4-^{t}BuPh	–1.09	0.15	1.24
^{t}Bu	Ph	–1.13	0.21	1.34

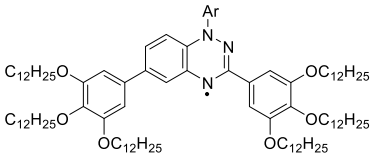

Ar	$E_{1/2}^{-1/0}$ (V)	$E_{1/2}^{0/+1}$ (V)	E_{cell} (V)
Ph	–1.14	0.22	1.25
3-FC_6H_4	–0.96	0.23	1.14
3,4,5-$(OC_{12}H_{25})_3C_6H_2$	–1.07	0.20	1.21
3,4,5-$(SC_{12}H_{25})_3C_6H_2$	–0.87	0.27	1.08

Figure 4. Specialized and structurally diverse Blatter radical derivatives and their redox potentials (vs Fc/Fc^+) in DCM.

3. Solvent and Electrolyte Effects on Redox Behavior of Blatter Radicals

A comparison of analogous systems measured in DCM and MeCN shows that reduction potentials ($E_{1/2}^{-1/0}$) shift markedly to more anodic values in the more polar solvent, while oxidation potentials ($E_{1/2}^{0/+1}$) shift only minimally. Consequently, switching from DCM to MeCN compresses the electrochemical gaps (ΔE_{cell}). For example, the C3-CF_3 substituted radical (Table 2, entries 22 vs 24; both taken from ref. 50), exhibits an anodic shift of +0.11 V for the reduction process, $E_{1/2}^{-1/0}$ = −1.12 V (DCM) to −1.01 V (MeCN), and a cathodic shift of only −0.04 V for oxidation, compressing ΔE_{cell} by −0.15 V (1.25 V to 1.10 V). Similarly, the C3-*t*-Bu analogue (entries 38 vs 39) shows an anodic $\Delta E_{1/2}^{-1/0}$ shift of +0.20 V for reduction, $E_{1/2}^{-1/0}$ = −1.49 V (DCM) to −1.29 V (MeCN), and a −0.03 V shift for oxidation, compressing ΔE_{cell} by −0.23 V (1.25 V to 1.02 V).

The relatively large anodic shift of the reduction process likely arises from solvent stabilization of the anionic state, either via polarization and/or hydrogen-bonding interactions. A similar compression effect of ΔE_{cell} was observed upon addition of water as co-solvent (Section 2.1, Table 1, entries 2 vs 3).[84] Notably, CV data collected in both MeCN and DMF (entries 83–88) gave very similar redox values for analogous radicals, despite the difference in polarity. However, the original values were reported vs Ag/AgCl, and the conversion to the Fc/Fc^+ scale used here is based on an assumed reference potential; thus, the apparent similarity should be regarded as approximate.

In contrast to solvent effects, the available data do not reveal a systematic effect of the supporting electrolyte. Direct comparison of measurements in DCM using *n*-Bu_4NPF_6 and *n*-Bu_4NBF_4 (*e.g.*, Table 2, entries 5 vs 6, 21–22 vs 23, 30 vs 31–32) shows no consistent directional trend in redox potentials, with variations typically ±0.10 V. This might suggest weak ion-pairing and negligible specific interactions between the electrolyte anions (PF_6^- vs BF_4^-) and the redox-active species; however, these comparisons derive from different studies and experimental conditions, and therefore do not permit a rigorous quantitative assessment of electrolyte effects. Thus, while the available data do not indicate a pronounced electrolyte-dependent shift in redox potentials, they are insufficient to draw firm conclusions. Other discrepancies observed for some compounds under similar but not strictly identical conditions (*e.g.*, Table 1, entries 1 vs 2 & 4 vs 5, Table 2 entries 21 vs 22 & 31 vs 32) are more likely attributable to experimental variables.[104–107]

The choice of supporting electrolyte, however, can affect the long-term stability of benzotriazinyl radicals in non-aqueous redox-flow batteries. In particular, the PF_6^- anion can decompose over extended periods (*ca.* 25 d), leading to capacity fade. Replacing it by tetrabutylammonium bis(trifluoromethanesulfonyl)imide (Bu_4NTFSI) dramatically improves longevity, retaining 87.5% of its initial capacity after 220 days.[112]

Table 2. Summary of electrochemical redox potentials of Blatter radicals as measured by cyclic voltammetry at *ca*. 20 °C with a scan rate of 50 or 100 mV·s^{-1}. Electrode configurations varied between studies; glassy carbon or Pt (working), Pt wire or foil counter electrodes and Ag/Ag$^+$ (e.g. Ag/AgCl, 1 M KCl) reference electrodes were commonly used; see specific electrochemical cell configuration in the source publication. Fc/Fc$^+$ or $FcMe_{10}/FcMe_{10}^+$ were used as internal references where reported. The redox potentials are stated as reported in the literature and converted vs Fc/Fc$^+$ (E_{Fc/Fc^+} = 0.0 V) where necessary. ΔE_{cell} values were calculated from unrounded potentials and rounded only for presentation

C7-Substituted

				Reported			*Referenced vs Fc/Fc$^+$*				
Entry	R^1	R^2	R^3	$E_{1/2}^{-1/0}$ (V)	$E_{1/2}^{0/+1}$ (V)	ΔE_{cell} (V)	$E_{1/2}^{-1/0}$ (V)	$E_{1/2}^{0/+1}$ (V)	ΔE_{cell} (V)	Solvent / Electrolyte	Ref.
1	Ph	Ph	H	−0.864	+0.288	1.152	−1.32	−0.17	1.15	DCM / *n*Bu$_4$NPF$_6$	15
2	Ph	Ph	H	−0.92	+0.28	1.20	−1.38	−0.18	1.20	DCM / *n*Bu$_4$NPF$_6$	16
3	Ph	Ph	H	−0.96	+0.10	1.06	−1.36	−0.30	1.06	MeCN / *n*Bu$_4$NBF$_4$	9
4	Ph	Ph	NC	−0.627	+0.543	1.170	−1.09	+0.08	1.17	DCM / *n*Bu$_4$NPF$_6$	15
5	Ph	Ph	F_3C	−0.700	+0.476	1.176	−1.16	+0.02	1.18	DCM / *n*Bu$_4$NPF$_6$	15
6	Ph	Ph	F_3C	−0.84	+0.36	1.20	−1.19	+0.01	1.20	DCM / *n*Bu$_4$NBF$_4$	13
7	Ph	Ph	F	−0.851	+0.281	1.132	−1.31	−0.18	1.13	DCM / *n*Bu$_4$NPF$_6$	15
8	Ph	Ph	Cl	−0.799	+0.361	1.160	−1.26	−0.10	1.16	DCM / *n*Bu$_4$NPF$_6$	15
9	Ph	Ph	Br	−0.772	+0.380	1.152	−1.23	−0.08	1.15	DCM / *n*Bu$_4$NPF$_6$	15
10	Ph	Ph	Br	−0.80	+0.31	1.11	−1.26	−0.15	1.11	DCM / *n*Bu$_4$NPF$_6$	113
11	Ph	Ph	I	−0.767	+0.366	1.133	−1.23	−0.09	1.13	DCM / *n*Bu$_4$NPF$_6$	15
12	Ph	Ph	4-FC_6H_4	−0.95	+0.16	1.11	−1.30	−0.19	1.11	DCM / *n*Bu$_4$NBF$_4$	59
13	Ph	Ph	Ph	−0.96	+0.15	1.11	−1.31	−0.20	1.11	DCM / *n*Bu$_4$NBF$_4$	59
14	Ph	Ph	$C_{10}H_8$	−0.83	+0.20	1.03	−1.29	−0.26	1.03	DCM / *n*Bu$_4$NPF$_6$	113
15	Ph	Ph	$C_{14}H_{10}$	−0.84	+0.19	1.03	−1.30	−0.27	1.03	DCM / *n*Bu$_4$NPF$_6$	113
16	Ph	Ph	$C{\equiv}CC_{14}H_{10}$	−0.80	+0.28	1.08	−1.26	−0.18	1.08	DCM / *n*Bu$_4$NPF$_6$	113
17	Ph	Ph	thien-2-yl	−0.95	+0.15	1.10	−1.30	−0.20	1.10	DCM / *n*Bu$_4$NBF$_4$	67
18	Ph	Ph	fur-2-yl	−0.96	+0.13	1.09	−1.31	−0.22	1.09	DCM / *n*Bu$_4$NBF$_4$	60
19	Ph	Ph	$C(Ph){=}CPh_2$	−1.27	−0.04	1.23	−1.27	−0.04	1.23	DCM / *n*Bu$_4$NPF$_6$	72
20	Ph	Ph	Me	−0.936	+0.193	1.129	−1.40	−0.27	1.13	DCM / *n*Bu$_4$NPF$_6$	15

C3-Substituted

				Reported			*Referenced vs Fc/Fc$^+$*				
Entry	R^1	R^2	R^3	$E_{1/2}^{-1/0}$ (V)	$E_{1/2}^{0/+1}$ (V)	ΔE_{cell} (V)	$E_{1/2}^{-1/0}$ (V)	$E_{1/2}^{0/+1}$ (V)	ΔE_{cell} (V)	Solvent / Electrolyte	Ref.
21	Ph	F_3C	H	−0.71	+0.58	1.29	−1.17	+0.12	1.29	DCM / nBu$_4$NPF$_6$	17
22	Ph	F_3C	H	−1.12	+0.13	1.25	−1.12	+0.13	1.25	DCM / nBu$_4$NPF$_6$	50
23	Ph	F_3C	H	−0.89	+0.25	1.14	−1.24	−0.10	1.14	DCM / nBu$_4$NBF$_4$	13
24	Ph	F_3C	H	−1.01	+0.09	1.10	−1.01	+0.09	1.10	MeCN / nBu$_4$NPF$_6$	50
25	Ph	F_3C	H	−1.03	+0.09	1.12	−1.03	+0.09	1.12	MeCN / nBu$_4$NPF$_6$	84
26	Ph	3-vinylC_6H_4	H	−0.831	+0.212	1.043	−1.23	−0.19	1.04	MeCN / nBu$_4$NPF$_6$	65
27	Ph	4-$O_2NC_6H_4$	H	−0.811	+0.365	1.176	−1.27	−0.10	1.18	DCM / nBu$_4$NPF$_6$	15
28	Ph	4-FC_6H_4	H	−0.97	+0.19	1.16	−1.32	−0.16	1.16	DCM / nBu$_4$NBF$_4$	13
29	Ph	pyrid-2-yl	H	−0.96	+0.21	1.17	−1.31	−0.14	1.17	DCM / nBu$_4$NBF$_4$	13
30	Ph	thien-2-yl	H	−0.823	+0.321	1.144	−1.28	−0.14	1.14	DCM / nBu$_4$NPF$_6$	15
31	Ph	thien-2-yl	H	−0.93	+0.19	1.12	−1.28	−0.16	1.12	DCM / nBu$_4$NBF$_4$	13
32	Ph	thien-2-yl	H	−0.88	+0.30	1.18	−1.34	−0.16	1.18	DCM / nBu$_4$NBF$_4$	17
33	Ph	C≡CPh	H	−0.78	+0.40	1.18	−1.24	−0.06	1.18	DCM / nBu$_4$NBF$_4$	17
34	Ph	4-[C(Ph)=CPh$_2$]C_6H_4	H	−1.27	+0.04	1.31	−1.27	+0.04	1.31	DCM / nBu$_4$NPF$_6$	72
35	Ph	ferrocenyl	H	–	+0.38	–	–	−0.08	–	DCM / nBu$_4$NPF$_6$	17
36	Ph	*t*-BuS	H	−0.90	+0.30	1.20	−1.36	−0.16	1.20	DCM / nBu$_4$NPF$_6$	17
37	Ph	Me	H	−1.06	+0.26	1.32	−1.41	−0.09	1.32	DCM / nBu$_4$NBF$_4$	13
38	Ph	*t*-Bu	H	−1.028	+0.218	1.246	−1.49	−0.24	1.25	DCM / nBu$_4$NPF$_6$	108
39	Ph	*t*-Bu	H	−1.29	−0.27	1.02	−1.29	−0.27	1.02	MeCN / nBu$_4$NPF$_6$	68
40	Ph	*n*-C_5H_{11}	H	−0.97	+0.24	1.21	−1.43	−0.22	1.21	DCM / nBu$_4$NPF$_6$	17
41	Ph	*c*-Pr	H	−1.008	+0.218	1.226	−1.47	−0.24	1.23	DCM / nBu$_4$NPF$_6$	108
42	Ph	*c*-Hex	H	−0.994	+0.218	1.212	−1.45	−0.24	1.21	DCM / nBu$_4$NPF$_6$	108
43	Ph	1-Ad	H	−1.06	+0.08	1.14	−1.41	−0.27	1.14	DCM / nBu$_4$NBF$_4$	13
44	Ph	NH_2	H	−0.96	+0.15	1.11	−1.42	−0.31	1.11	DCM / nBu$_4$NPF$_6$	17
45	Ph	morpholin-4-yl	H	−0.98	+0.08	1.06	−1.44	−0.38	1.06	DCM / nBu$_4$NPF$_6$	17
46	Ph	piperidin-1-yl	H	−1.001	+0.021	1.022	−1.46	−0.44	1.02	DCM / nBu$_4$NPF$_6$	108
47	Ph	pyrrolidin-1-yl	H	−1.021	+0.012	1.033	−1.48	−0.45	1.03	DCM / nBu$_4$NPF$_6$	108
48	Ph	NMePh	H	−0.921	+0.088	1.009	−1.38	−0.37	1.01	DCM / nBu$_4$NPF$_6$	108
49	Ph	NHPh	H	−1.025	−0.118	0.907	−1.03	−0.12	0.91	MeCN / nBu$_4$NPF$_6$	90

C3-Substituted. *Continued*

Entry	R^1	R^2	R^3	$E_{1/2}^{-1/0}$ (V)	$E_{1/2}^{0/+1}$ (V)	ΔE_{cell} (V)	$E_{1/2}^{-1/0}$ (V)	$E_{1/2}^{0/+1}$ (V)	ΔE_{cell} (V)	Solvent / Electrolyte	Ref.
50	Ph	NHPh	H	−1.21	−0.32	0.89	−1.21	−0.32	0.89	MeCN / nBu$_4$NPF$_6$	18
51	Ph	NHPh	H	−1.24	−0.31	0.93	−1.24	−0.31	0.93	MeCN / nBu$_4$NPF$_6$	84
52	Ph	N(CHO)Ph	H	−0.933	+0.029	0.962	−0.93	+0.03	0.96	MeCN / nBu$_4$NPF$_6$	90
53	Ph	N(CHO)Ph	H	−1.06	−0.11	0.95	−1.06	−0.11	0.95	MeCN / nBu$_4$NPF$_6$	18
54	Ph	N(CHO)Ph	H	−1.07	−0.09	0.98	−1.07	−0.09	0.98	MeCN / nBu$_4$NPF$_6$	84

N1-Substituted

				Reported			*Referenced vs Fc/Fc$^+$*				
Entry	R^1	R^2	R^3	$E_{1/2}^{-1/0}$ (V)	$E_{1/2}^{0/+1}$ (V)	ΔE_{cell} (V)	$E_{1/2}^{-1/0}$ (V)	$E_{1/2}^{0/+1}$ (V)	ΔE_{cell} (V)	Solvent / Electrolyte	Ref.
55	C_6F_5	Ph	H	−0.757	+0.565	1.322	−1.22	+0.11	1.32	DCM / nBu$_4$NPF$_6$	15
56[a]	2,3,5,6-F_4C_6H	Ph	H	−0.682	+0.484	1.166	−1.08	+0.08	1.17	MeCN / nBu$_4$NBF$_4$	109
57[a]	2,3,4-$F_3C_6H_2$	Ph	H	−0.728	+0.362	1.090	−1.13	−0.04	1.09	MeCN / nBu$_4$NBF$_4$	109
58[a]	2,4-$F_2C_6H_3$	Ph	H	−0.766	+0.336	1.102	−1.17	−0.06	1.10	MeCN / nBu$_4$NBF$_4$	109
59[a]	3,4-$F_2C_6H_3$	Ph	H	−0.709	+0.295	1.004	−1.11	−0.10	1.00	MeCN / nBu$_4$NBF$_4$	109
60	4-NCC_6H_4	Ph	H	−0.78	+0.28	1.06	−1.13	−0.07	1.06	DCM / nBu$_4$NBF$_4$	13
61	pyrid-2-yl	Ph	H	−0.76	+0.34	1.10	−1.22	−0.12	1.10	DCM / nBu$_4$NBF$_4$	16
62	pyrid-2-yl	Ph	H	−0.82	+0.24	1.06	−1.17	−0.11	1.06	DCM / nBu$_4$NBF$_4$	13
63	2-$MeOC_6H_4$	Ph	H	−1.01	+0.24	1.25	−1.47	−0.22	1.25	DCM / nBu$_4$NPF$_6$	16
64	4-[C(Ph)=CPh$_2$]C_6H_4	Ph	H	−1.28	−0.08	1.20	−1.28	−0.08	1.20	DCM / nBu$_4$NPF$_6$	72

[a] Calculated assuming $E_{Fc/Fc+}$ = 0.40 V *vs* Ag/AgCl in MeCN, due to the absence of an internal Fc calibrant in the primary literature. Treat as comparative estimates.

Synergistic effects

				Reported			*Referenced vs Fc/Fc⁺*				
Entry	R^1	R^2	R^3	$E_{1/2}^{-1/0}$ (V)	$E_{1/2}^{0/+1}$ (V)	ΔE_{cell} (V)	$E_{1/2}^{-1/0}$ (V)	$E_{1/2}^{0/+1}$ (V)	ΔE_{cell} (V)	Solvent / Electrolyte	Ref.
65	Ph	Me	F_3C	−0.84	+0.35	1.19	−1.19	+0.00	1.19	DCM / nBu$_4$NBF$_4$	13
66	Ph	F_3C	F_3C	−0.58	+0.66	1.24	−0.93	+0.31	1.24	DCM / nBu$_4$NBF$_4$	13
67	Ph	*t*-Bu	F_3C	−1.11	−0.04	1.07	−1.11	−0.04	1.07	DCM / nBu$_4$NPF$_6$	68
68	Ph	pyrid-2-yl	F_3C	−0.85	+0.31	1.16	−0.85	+0.31	1.16	DCM / nBu$_4$NPF$_6$	29
69	Ph	pyrid-2-yl	Cl	−0.97	+0.19	1.16	−0.97	+0.19	1.16	DCM / nBu$_4$NPF$_6$	31
70	Ph	pyrid-2-yl	Br	−0.91	+0.22	1.13	−0.91	+0.22	1.13	DCM / nBu$_4$NPF$_6$	31
71	Ph	pyrid-2-yl	I	−0.95	+0.18	1.13	−0.95	+0.18	1.13	DCM / nBu$_4$NPF$_6$	31
72	Ph	4-Tol	F_3C	−0.710	+0.462	1.172	−1.17	+0.00	1.17	DCM / nBu$_4$NPF$_6$	15
73	Ph	4-Tol	I	−0.783	+0.350	1.133	−1.24	−0.11	1.13	DCM / nBu$_4$NPF$_6$	15
74	Ph	4-FC_6H_4	F_3C	−0.704	+0.474	1.178	−1.16	+0.01	1.18	DCM / nBu$_4$NPF$_6$	15
75	Ph	4-FC_6H_4	I	−0.781	+0.356	1.137	−1.24	−0.10	1.14	DCM / nBu$_4$NPF$_6$	15
76	Ph	thien-2-yl	F_3C	−0.680	+0.488	1.168	−1.14	+0.03	1.17	DCM / nBu$_4$NPF$_6$	15
77	Ph	thien-2-yl	CN	−0.598	+0.555	1.153	−1.06	+0.10	1.15	DCM / nBu$_4$NPF$_6$	15
78	Ph	thien-2-yl	I	−0.703	+0.420	1.123	−1.16	−0.04	1.12	DCM / nBu$_4$NPF$_6$	15
79	C_6F_5	Ph	F_3C	−0.522	+0.796	1.318	−0.98	+0.34	1.32	DCM / nBu$_4$NPF$_6$	15
80	C_6F_5	thien-2-yl	F_3C	−0.480	+0.817	1.297	−0.94	+0.36	1.30	DCM / nBu$_4$NPF$_6$	15
81	4-BrC_6H_4	3-vinylC_6H_4	H	−0.769	+0.249	1.018	−1.17	−0.15	1.02	MeCN / nBu$_4$NPF$_6$	65
82	4-NCC_6H_4	thien-2-yl	H	−0.67	+0.33	1.00	−1.02	−0.02	1.00	DCM / nBu$_4$NBF$_4$	13
83[b]	2,3,6-$F_3C_6H_2$	4-FC_6H_4	H	−0.954	+0.231	1.185	−1.41	−0.23	1.19	MeCN / nBu$_4$NPF$_6$	97
84[b]	2,3,6-$F_3C_6H_2$	4-FC_6H_4	H	−0.952	+0.240	1.192	−1.41	−0.22	1.19	DMF / nBu$_4$NPF$_6$	97
85[b]	2,3,5,6-F_4C_6H	4-FC_6H_4	H	−0.896	+0.270	1.166	−1.36	−0.19	1.17	MeCN / nBu$_4$NPF$_6$	97

Synergistic effects. Continued

Entry	R^1	R^2	R^3	$E_{1/2}^{-1/0}$ (V)	$E_{1/2}^{0/+1}$ (V)	ΔE_{cell} (V)	$E_{1/2}^{-1/0}$ (V)	$E_{1/2}^{0/+1}$ (V)	ΔE_{cell} (V)	Solvent / Electrolyte	Ref.
86[b]	2,3,5,6-F_4C_6H	4-FC_6H_4	H	−0.934	+0.234	1.168	−1.39	−0.23	1.17	DMF / nBu$_4$NPF$_6$	97
87[b]	C_6F_5	4-FC_6H_4	H	−0.888	+0.278	1.166	−1.35	−0.18	1.17	MeCN / nBu$_4$NPF$_6$	97
88[b]	C_6F_5	4-FC_6H_4	H	−0.885	+0.275	1.160	−1.35	−0.19	1.16	DMF / nBu$_4$NPF$_6$	97
89	Ph	4-$MeO_2CC_6H_4$	$C_2H_4CO_2H$	−0.61	+0.55	1.16	−0.61	+0.55	1.16	DCM / nBu$_4$NPF$_6$	32
90	Ph	4-$HO_2CC_6H_4$	CO_2H	−0.85	+0.17	1.02	−0.85	+0.17	1.02	DCM / nBu$_4$NPF$_6$	32
91	4-$EtCO_2CC_6H_4$	4-$MeO_2CC_6H_4$	$C_2H_4CO_2H$	−0.48	+0.58	1.06	−0.48	+0.58	1.06	DCM / nBu$_4$NPF$_6$	32
92	4-$HO_2CC_6H_4$	4-$HO_2CC_6H_4$	CO_2H	−0.85	+0.13	0.98	−0.85	+0.13	0.98	DCM / nBu$_4$NPF$_6$	32
93	4-$MeOC_6H_4$	F_3C	H	−1.09	+0.05	1.14	−1.09	+0.05	1.14	MeCN / nBu$_4$NPF$_6$	84
94	4-$H_2NC_6H_4$	F_3C	H	−1.15	−0.06	1.09	−1.15	−0.06	1.09	MeCN / nBu$_4$NPF$_6$	84
95	4-FC_6H_4	F_3C	H	−1.02	+0.12	1.14	−1.02	+0.12	1.14	MeCN / nBu$_4$NPF$_6$	84
96	4-$F_3CC_6H_4$	F_3C	H	−0.87	+0.17	1.04	−0.87	+0.17	1.04	MeCN / nBu$_4$NPF$_6$	84
97	4-$O_2NC_6H_4$	F_3C	H	−0.71	+0.20	0.91	−0.71	+0.20	0.91	MeCN / nBu$_4$NPF$_6$	84
98	4-$HO_2CC_6H_4$	F_3C	H	−1.04	+0.24	1.28	−1.04	+0.24	1.28	MeCN / nBu$_4$NPF$_6$	84
99	2,6-$Cl_2C_6H_3$	F_3C	H	−0.99	+0.32	1.31	−0.99	+0.32	1.31	MeCN / nBu$_4$NPF$_6$	84

[b] Calculated assuming $E_{Fc/Fc+}$ = 0.46 V *vs* Ag/AgCl in MeCN and in DMF, due to absence of internal Fc calibrant in the primary literature. Treat as comparative estimates.

4. Brief Comparison with Other Persistent Organic Radical Families

Classical persistent organic radicals, such as nitroxides,[114] triarylmethyl,[115] and phenalenyl[116] systems, derive their stability primarily from a combination of spin delocalization and kinetic protection via steric hindrance[117] (Table 3). For instance, nitroxides like TEMPO are prized for their reversible oxidation ($E_{1/2}^{0/+1}$ ~ +0.3 V vs Fc/Fc$^+$),[118–119] yet they typically exhibit irreversible or inaccessible reductions at highly cathodic potentials (~−1.5 V vs Fc/Fc$^+$), limiting their use in ambipolar applications as their electrochemical gap is often too large (ΔE_{cell} ~1.5–2.3 V) (Table 3, Nitroxides). Similarly, thiazyl radicals[120] rely on heteroatom stabilization, but often face challenges related to dimerization or limited structural modularity, with relatively narrow electrochemical windows (ΔE_{cell} ~1–1.5 V) (Table 3, Thiazyls). In contrast, benzotriazinyl (Blatter) radicals exhibit a remarkable form of intrinsic thermodynamic stabilization arising from extensive π-delocalization across a nitrogen-rich, heterocyclic framework. Compared to verdazyls,[121–123] which are also N-centered and highly stable, Blatter radicals offer a particularly attractive combination of reversible ambipolar electrochemistry, and substituent-dependent tuning of both oxidation and reduction potentials. While verdazyls generally exhibit electrochemical windows of 1.0–1.6 V, their redox potentials are comparatively less tunable (Table 3, Verdazyls).[121] Blatter

radicals provide a robust platform with tunable redox potentials and relatively narrow electrochemical gaps (ΔE_{cell} ~1–1.4 V) (Table 3, Blatter radicals). Ultimately, the combination of high thermodynamic stability, reversible ambipolar redox behavior, and modular electronic tunability distinguishes benzotriazinyl radicals as a uniquely versatile platform for functional materials.

Table 3. Representative redox potentials of selected persistent organic radical families

Radical Class	$E_{1/2}{}^{-1/0}$ (V)	$E_{1/2}{}^{0/+1}$ (V)	ΔE_{cell} (V)	General Characteristics
Nitroxides (*e.g.*, TEMPO)	−2.0 to −1.5[a]	+0.1 to +0.5	~1.5–2.3	*p*-type (Oxidation)
Triarylmethyls (TAM)	−1.1 to −0.7	+0.5 to +0.8	~1.2–1.8	Dual, but sterically bulky
Phenalenyls	−1.6 to −1.2	−0.3 to +0.1	~0.9–1.4	Limited data, unstable
Thiazyls	−1.0 to −0.4	+0.2 to +0.8	~0.9–1.5	Often prone to dimerization
Verdazyls	−1.4 to −0.9	−0.1 to +0.4	~1.0–1.6	Stable, less tunable derivatives
Blatter radicals	−1.5 to −0.5	−0.5 to +0.6	~1.0–1.4	Stable, tunable redox, narrow window

[a] Reduction is frequently irreversible and values should be regarded as approximate reported reduction potentials rather than true reversible $E_{1/2}$ values.
Note: Values are representative ranges compiled from commonly studied derivatives and are intended for qualitative comparison only. Reported potentials originate from different studies employing different solvents, supporting electrolytes, and reference electrodes (commonly converted to Fc/Fc^+ where possible), and therefore should not be interpreted as rigorously normalized electrochemical data.

5. Conclusions

Blatter radicals represent a unique class of persistent heteroaromatic radicals, distinguished by their robust and highly reversible bipolar electrochemistry. Delocalization stabilizes both oxidized and reduced states, resulting in relatively small electrochemical gaps (~1–1.5 V). Redox properties can be tuned through strategic substitutions at key positions, while structural modifications offer an additional layer of control. Substitution at electronically-active positions, particularly C3, enables substantial modulation of both redox potentials, while weaker coupling at C7 and N1, and electronic insulation at C5/C6, allow more selective or minimal perturbation. The combined effects of substituents define distinct regimes of electrochemical behavior, ranging from gap expansion in electron-withdrawing systems to gap compression in donor–acceptor architectures. Environmental conditions, particularly solvent polarity, further influence reduction potentials, underscoring the scaffold's versatility for molecular design. Exceptional stability and tunable redox profiles of Blatter radicals are actively driving applications in organic redox-flow batteries, molecular electronics, and spin-based devices. Future efforts should focus on tailoring electrochemical gaps and redox potentials to the requirements of specific applications, to fully realize their potential in next-generation organic electronics.

The electrochemical data compiled in this review are generally of high quality, with most studies employing internal Fc/Fc^+ (or equivalent) referencing and reporting reversible behavior. Nevertheless, variations in

experimental conditions, including solvent, supporting electrolyte, reference electrode, scan rate, and instrumentation (e.g., IR compensation), introduce inherent variability in absolute redox potentials. Consequently, the trends and design principles discussed herein should be interpreted as robust qualitative relationships rather than strictly quantitative correlations.

Acknowledgements

The author acknowledges funding from the project POST-DOC/0524/0150, which is implemented under the programme of social cohesion "THALIA 2021-2027" co-funded by the European Union, through Research and Innovation Foundation.

Supplementary Material

Computational methodology and Cartesian coordinates for the calculations used to generate the molecular orbital plots shown in Figure 3 are provided in the Supporting Information.

References

1. Blatter, H. M.; Lukaszewski, H. *Tetrahedron Lett*. **1968**, *9*, 2701. https://doi.org/10.1016/S0040-4039(00)89678-1
2. Huisgen, R.; Wulff, J. *Chem. Ber*. **1969**, *102*, 1848. https://doi.org/10.1002/cber.19691020609
3. Gubaidullin, A. T.; Buzykin, B. I.; Litvinov, I. A.; Gazetdinova, N. A. *Russ. J. Gen. Chem.* **2004**, *74*, 939. https://doi.org/10.1023/B:RUGC.0000042432.08612.2a
4. Neugebauer, F. A.; Umminger, I. *Chem. Ber.* **1980**, *113*, 1205. https://doi.org/10.1002/cber.19801130402
5. Neugebauer, F. A.; Umminger, I. *Chem. Ber*. **1981**, *114*, 2423. https://doi.org/10.1002/cber.19811140709
6. Neugebauer, F. A.; Rimmler, G. *Magn. Reson. Chem.* **1988**, *26*, 595. https://doi.org/10.1002/mrc.1260260712
7. Kadirov, M. K.; Il'yasov, A. V.; Vafina, A. A.; Buzykin, B. I.; Gazetdinova, N. G.; Kitaev, Y. P. *Bull. Acad. Sci. USSR, Div. Chem. Sci.* **1984**, *33*, 649. https://doi.org/10.1007/BF00995717
8. Mukai, K.; Inoue, K.; Achiwa, N.; Jamali, J. B.; Krieger, C.; Neugebauer, F. A. *Chem. Phys. Lett.* **1994**, *224*, 569. https://doi.org/10.1016/0009-2614(94)00586-9
9. Hutchison, K. A.; Srdanov, G.; Menon, R.; Gabriel, J.-C. P.; Knight, B.; Wudl, F. *J. Am. Chem. Soc.* **1996**, *118*, 13081. https://doi.org/10.1021/ja963174i
10. Krieger, C.; Neugebauer, F. A. *Acta Cryst.* **1996**, *C52*, 3124.

https://doi.org/10.1107/S0108270196011092
11. Kadirov, M. K.; Buzykin, B. I.; Gazetdinova, N. G. *Russ. Chem. Bull.* **2002**, *51*, 1796. https://doi.org/10.1023/A:1021331930462
12. Koutentis, P. A.; Lo Re, D. *Synthesis* **2010**, 2075. https://doi.org/10.1055/s-0029-1218782
13. Berezin, A. A.; Zissimou, G.; Constantinides, C. P.; Beldjoudi, Y.; Rawson, J. M.; Koutentis, P. A. *J. Org. Chem.* **2014**, *79*, 314. https://doi.org/10.1021/jo402481t
14. Constantinides, C. P.; Berezin, A. A.; Zissimou, G. A.; Manoli, M.; Leitus, G. M.; Bendikov, M.; Probert, M. R.; Rawson, J. M.; Koutentis, P. A. *J. Am. Chem. Soc.* **2014**, *136*, 11906. https://doi.org/10.1021/ja5063746
15. Savva, A. C.; Mirallai, S. I.; Zissimou, G. A.; Berezin, A. A.; Demetriades, M.; Kourtellaris, A.; Constantinides, C. P.; Nicolaides, C.; Trypiniotis, T.; Koutentis, P. A. *J. Org. Chem.* **2017**, *82*, 7564. https://doi.org/10.1021/acs.joc.7b01297
16. Constantinides, C. P.; Obijalska, E.; Kaszyński, P. *Org. Lett.* **2016**, *18*, 916. https://doi.org/10.1021/acs.orglett.5b03528
17. Pomikło, D.; Bodzioch, A.; Pietrzak, A.; Kaszyński, P. *Org. Lett*. **2019**, *21*, 6995. https://doi.org/10.1021/acs.orglett.9b02563
18. Grant, J. A.; Lu, Z.; Tucker, D. E.; Hockin, B. M.; Yufit, D. S.; Fox, M. A.; Kataky, R.; Chechik, V.; O'Donoghue, A. C. *Nat. Commun*. **2017**, *8*, 15088. https://doi.org/10.1038/ncomms15088
19. Bodzioch, A.; Zheng, M.; Kaszyński, P.; Utecht, G. *J. Org. Chem*. **2014**, *79*, 7294. https://doi.org/10.1021/jo500898e
20. Constantinides, C. P.; Koutentis, P. A.; Loizou, G. *Org. Biomol. Chem*. **2011**, *9*, 3122. https://doi.org/10.1039/C1OB05167A
21. Takahashi, Y.; Miura, Y.; Yoshioka, N. *Chem. Lett.* **2014**, *43*, 1236. https://doi.org/10.1246/cl.140335
22. Berezin, A. A.; Koutentis, P. A. *Org. Biomol. Chem*. **2014**, *12*, 1641. https://doi.org/10.1039/C3OB42130A
23. Koutentis, P. A.; Krassos, H.; Lo Re, D. *Org. Biomol. Chem.* **2011**, *9*, 5228. https://doi.org/10.1039/c1ob05410d
24. Berezin, A. A.; Constantinides, C. P.; Drouza, C.; Manoli, M.; Koutentis, P. A. *Org. Lett.* **2012**, *14*, 5586. https://doi.org/10.1021/ol302714j
25. Berezin, A. A.; Constantinides, C. P.; Mirallai, S. I.; Manoli, M.; Cao, L. L.; Rawson, J. M.; Koutentis, P. A. *Org. Biomol. Chem.* **2013**, *11*, 6780. https://doi.org/10.1039/C3OB41169A
26. Morgan, I. S.; Peuronen, A.; Hänninen, M. M.; Reed, R. W.; Clérac, R.; Tuononen, H. M. *Inorg. Chem*. **2014**, *53*, 33. https://doi.org/10.1021/ic402954p
27. Morgan, I. S.; Mansikkamäki, A.; Zissimou, G. A.; Koutentis, P. A.; Rouzières, M.; Clérac, R.; Tuononen, H. M. *Chem. – Eur. J.* **2015**, *21*, 15843. https://doi.org/10.1002/chem.201501343

28. Morgan, I. S.; Mansikkamäki, A.; Rouzières, M.; Clérac, R.; Tuononen, H. M. *Dalton Trans.* **2017**, *46*, 12790. https://doi.org/10.1039/C7DT02766D
29. Nasani, R.; Sidharth, T. N. S.; Roy, S.; Mondal, A.; Rawson, J. M.; Konar, S. *Dalton Trans.* **2019**, *48*, 14189. https://doi.org/10.1039/C9DT01918A
30. Sidharth, T. N. S.; Nasani, R.; Gupta, A.; Sooraj, B. N. S.; Roy, S.; Mondal, A.; Konar, S. *Inorg. Chim. Acta* **2020**, *503*, 119395. https://doi.org/10.1016/j.ica.2019.119395
31. Kapurwan, S.; Gupta, A.; Mondal, A.; Konar, S. *ChemistrySelect* **2022**, *7*, e202104536. https://doi.org/10.1002/slct.202104536
32. Qu, L.; Chen, H.; Shi, C.; Li, H.; Ai, Q.; Liu, X.; Yang, C.; Yang, H.; Hu, X. *New J. Chem*. **2022**, *46*, 21366. https://doi.org/10.1039/D2NJ03772F
33. Jasiński, M.; Szczytko, J.; Pociecha, D.; Monobe, H.; Kaszyński, P. *J. Am. Chem. Soc.* **2016**, *138*, 9421. https://doi.org/10.1021/jacs.6b06444
34. Jasiński, M.; Szymańska, K.; Gardias, A.; Pociecha, D.; Monobe, H.; Szczytko, J.; Kaszyński, P. *ChemPhysChem* **2019**, *20*, 636. https://doi.org/10.1002/cphc.201800965
35. Jasiński, M.; Kapuściński, S.; Kaszyński, P. *J. Mol. Liq.* **2019**, *277*, 1054. https://doi.org/10.1016/j.molliq.2019.01.014
36. Kapuściński, S.; Gardias, A.; Pociecha, D.; Jasiński, M.; Szczytko, J.; Kaszyński, P. *J. Mater. Chem. C* **2018**, *6*, 3079. https://doi.org/10.1039/C8TC00487K
37. Kaszyński, P.; Kapuściński, S.; Ciastek-Iskrzycka, S. In *Advances in Heterocyclic Chemistry*; Scriven, E. F. V.; Ramsden, C. A. Eds.; Academic Press: Amsterdam, 2019; Vol. 128, pp 263–331. https://doi.org/10.1016/bs.aihch.2019.01.001
38. Shivakumar, K. I.; Pociecha, D.; Szczytko, J.; Kapuściński, S.; Monobe, H.; Kaszyński, P. *J. Mater. Chem. C* **2020**, *8*, 1083. https://doi.org/10.1039/C9TC05764A
39. Kaszyński, P.; Constantinides, C. P.; Young, V. G. *Angew. Chem. Int. Ed*. **2016**, *55*, 11149. https://doi.org/10.1002/anie.201605612
40. Bartos, P.; Anand, B.; Pietrzak, A.; Kaszyński, P. *Org. Lett.* **2020**, *22*, 180. https://doi.org/10.1021/acs.orglett.9b04130
41. Bartos, P.; Young, V. G. Jr.; Kaszyński, P. *Org. Lett.* **2020**, *22*, 3835. https://doi.org/10.1021/acs.orglett.0c01074
42. Hande, A. A.; Darrigan, C.; Bartos, P.; Baylère, P.; Pietrzak, A.; Kaszyński, P.; Chrostowska, A. *Phys. Chem. Chem. Phys.* **2020**, *22*, 23637. https://doi.org/10.1039/D0CP03896B
43. Bartos, P.; Celeda, M.; Pietrzak, A.; Kaszyński, P. *Org. Chem. Front.* **2022**, *9*, 929. https://doi.org/10.1039/D1QO01742J
44. Zissimou, G. A.; Bartos, P.; Pietrzak, A.; Kaszyński, P. *J. Org. Chem*. **2022**, *87*, 4829. https://doi.org/10.1021/acs.joc.2c00178
45. Bartos, P.; Szamweber, P.; Camargo, B.; Pietrzak, A.; Kaszyński, P. *Chem. Sci*. **2025**, *16*, 12139. https://doi.org/10.1039/D5SC01182E

46. Singh, H. S.; Zissimou, G. A.; Pociecha, D.; Cigl, M.; Pietrzak, A.; Kaszyński, P. *J. Mater. Chem. C* **2025**, *13*, 19285. https://doi.org/10.1039/D5TC02401C
47. Singh, H. K.; Bodzioch, A.; Pietrzak, A.; Kaszyński, P. *Chem. Commun*. **2025**, *61*, 496. https://doi.org/10.1039/D4CC05704J
48. Zhang, S.; Pink, M.; Junghoefer, T.; Zhao, W.; Hsu, S.-N.; Rajca, S.; Calzolari, A.; Boudouris, B. W.; Casu, M. B.; Rajca, A. *J. Am. Chem. Soc*. **2022**, *144*, 6059. https://doi.org/10.1021/jacs.2c01141
49. Pomikło, D.; Pietrzak, A.; Kishi, R.; Kaszyński, P. *Mater. Chem. Front*. **2023**, *7*, 4928. https://doi.org/10.1039/D3QM00666B
50. Pomikło, D.; Kaszyński, P. *Chem. – Eur. J.* **2023**, *29*, e202301069. https://doi.org/10.1002/chem.202301069
51. Bartos, P.; Pomikło, D.; Sorenson, K. D.; Hietsoi, O.; Friedli, A. C.; Kaszyński, P. *J. Am. Chem. Soc*. **2025**, *147*, 125. https://doi.org/10.1021/jacs.4c16500
52. Zissimou, G. A.; Berezin, A. A.; Manoli, M.; Nicolaides, C.; Trypiniotis, T.; Koutentis, P. A. *Tetrahedron* **2020**, *76*, 131077. https://doi.org/10.1016/j.tet.2020.131077
53. Boudalis, A. K.; Constantinides, C. P.; Chrysochos, N.; Carmieli, R.; Leitus, G.; Kourtellaris, A.; Lawson, D. B.; Koutentis, P. A. *J. Magn. Reson.* **2023**, *349*, 107406. https://doi.org/10.1016/j.jmr.2023.107406
54. Aoki, T.; Sotome, H.; Shimizu, D.; Miyasaka, H.; Matsuda, K. *Angew. Chem., Int. Ed*. **2025**, *64*, e202418655. https://doi.org/10.1002/anie.202418655
55. Duan, J.-J.; Yang, X.-Q.; Berezin, A.; Zissimou, G. A.; Koutentis, P. A.; Li, R.-N.; Luo, G.; Wang, S.-F.; Wang, Y.-F.; Chen, T.; Wang, D. *ACS Nano* **2025**, *19*, 34981. https://doi.org/10.1021/acsnano.5c11549
56. Tretyakov, E. V.; Zayakin, I. A.; Dmitriev, A. A.; Fedin, M. V.; Romanenko, G. V.; Bogomyakov, A. S.; Akyeva, A. Y.; Syroeshkin, M. A.; Yoshioka, N.; Gritsan, N. P. *Chem. – Eur. J*. **2024**, *30*, e202303456. https://doi.org/10.1002/chem.202303456
57. Karecla, G.; Papagiorgis, P.; Panagi, N.; Zissimou, G. A.; Constantinides, C. P.; Koutentis, P. A.; Itskos, G.; Hayes, S. C. *New J. Chem*. **2017**, *41*, 8604. https://doi.org/10.1039/C7NJ00677B
58. Bar-David, J.; Daaoub, A.; Chen, S.; Sibug-Torres, S. M.; Rocchetti, S.; Kang, G.; Davidson, R. J.; Salthouse, R. J.; Guo, C.; Mueller, N. S.; Sangtarash, S.; Bryce, M. R.; Sadeghi, H.; Baumberg, J. J. *ACS Nano* **2025**, *19*, 7650. https://doi.org/10.1021/acsnano.4c09661
59. Constantinides, C. P.; Koutentis, P. A.; Rawson, J. M. *Chem. – Eur. J*. **2012**, *18*, 15433. https://doi.org/10.1002/chem.201202784
60. Constantinides, C. P.; Carter, E.; Murphy, D. M.; Manoli, M.; Leitus, G. M.; Bendikov, M.; Rawson, J. M.; Koutentis, P. A. *Chem. Commun*. **2013**, *49*, 8662. https://doi.org/10.1039/C3CC44899A
61. Miura, Y.; Yoshioka, N. *Chem. Phys. Lett.* **2015**, *626*, 11.

https://doi.org/10.1016/j.cplett.2015.03.009
62. Constantinides, C. P.; Lawson, D. B.; Zissimou, G. A.; Berezin, A. A.; Mailman, A.; Manoli, M.; Kourtellaris, A.; Leitus, G. M.; Clérac, R.; Tuononen, H. M.; Koutentis, P. A. *CrystEngComm*. **2020**, *22*, 5453. https://doi.org/10.1039/D0CE00789G
63. Bazzi, F.; Danke, A. J.; Lawson, D. B.; Manoli, M.; Leitus, G. M.; Koutentis, P. A.; Constantinides, C. P. *CrystEngComm*. **2020**, *22*, 4306. https://doi.org/10.1039/D0CE00669F
64. Constantinides, C. P.; Berezin, A. A.; Manoli, M.; Leitus, G. M.; Zissimou, G. A.; Bendikov, M.; Rawson, J. M.; Koutentis, P. A. *Chem. – Eur. J.* **2014**, *20*, 5388. https://doi.org/10.1002/chem.201304538
65. Yan, B.; Cramen, J.; McDonald, R.; Frank, N. L. *Chem. Commun*. **2011**, *47*, 3201. https://doi.org/10.1039/C0CC04727A
66. Constantinides, C. P.; Koutentis, P. A.; Krassos, H.; Rawson, J. M.; Tasiopoulos, A. J. *J. Org. Chem*. **2011**, *76*, 2798. https://doi.org/10.1021/jo200210s
67. Constantinides, C. P.; Koutentis, P. A.; Rawson, J. M. *Chem. – Eur. J*. **2012**, *18*, 7109. https://doi.org/10.1002/chem.201200248
68. Takahashi, Y.; Miura, Y.; Yoshioka, N. *New J. Chem*. **2015**, *39*, 4783. https://doi.org/10.1039/C5NJ00393H
69. Gardias, A.; Kaszyński, P.; Obijalska, E.; Trzybiński, D.; Domagała, S.; Woźniak, K.; Szczytko, J. *Chem. – Eur. J*. **2018**, *24*, 1317. https://doi.org/10.1002/chem.201703576
70. Constantinides, C. P.; Lawson, D. B.; Berezin, A. A.; Zissimou, G. A.; Manoli, M.; Leitus, G. M.; Koutentis, P. A. *CrystEngComm*. **2019**, *21*, 4599. https://doi.org/10.1039/C9CE00739C
71. Takahashi, Y.; Tsuchiya, N.; Miura, Y.; Yoshioka, N. *New J. Chem*. **2018**, *42*, 9949. https://doi.org/10.1039/C7NJ04534D
72. Hu, X.; Chen, H.; Zhao, L.; Miao, M.; Zheng, Y. *Chem. Mater*. **2019**, *31*, 10256. https://doi.org/10.1021/acs.chemmater.9b04495
73. Fumanal, M.; Vela, S.; Ribas-Ariño, J.; Novoa, J. J. *Chem. – Asian J.* **2014**, *9*, 3612. https://doi.org/10.1002/asia.201402871
74. Fumanal, M.; Vela, S.; Novoa, J. J.; Ribas-Ariño, J. *Chem. Commun*. **2015**, *51*, 15776. https://doi.org/10.1039/C5CC06288H
75. Ciccullo, F.; Gallagher, N. M.; Geladari, O.; Chassé, T.; Rajca, A.; Casu, M. B. *ACS Appl. Mater. Interfaces* **2016**, *8*, 1805. https://doi.org/10.1021/acsami.5b09693
76. Constantinides, C. P.; Berezin, A. A.; Zissimou, G. A.; Manoli, M.; Leitus, G. M.; Koutentis, P. A. *Molecules* **2016**, *21*, 636. https://doi.org/10.3390/molecules21050636
77. Demetriou, M.; Berezin, A. A.; Koutentis, P. A.; Krasia-Christoforou, T. *Polym. Int.* **2013**, *63*, 674. https://doi.org/10.1002/pi.4566
78. Kuznetsova, Y. L.; Vavilova, A. S.; Malysheva, Y. B.; Lopatin, M. A.; Grishin, I. D.; Burdyukova, T. O.; Zaburdaeva, E. A.; Polozov, E. Yu.; Fedorov, A. Yu. *Russ. Chem. Bull.* **2020**, *69*, 1470.

https://doi.org/10.1007/s11172-020-2925-1
79. Areephong, J.; Treat, N.; Kramer, J. W.; Christianson, M. D.; Hawker, C. J.; Collins, H. A. PCT Int. Appl. 2015 061189, 2015.
80. Areephong, J.; Mattson, K. M.; Treat, N. J.; Poelma, S. O.; Kramer, J. W.; Sprafke, H. A.; Latimer, A. A.; Read de Alaniz, J.; Hawker, C. J. *Polym. Chem.* **2016**, *7*, 370. https://doi.org/10.1039/c5py01563d
81. Zheng, Y.; Miao, M.-S.; Kemei, M. C.; Seshadri, R.; Wudl, F. *Isr. J. Chem.* **2014**, *54*, 774. https://doi.org/10.1002/ijch.201400034
82. Poryvaev, A. S.; Polyukhov, D. M.; Gjuzi, E.; Hoffmann, F.; Fröba, M.; Fedin, M. V. *Inorg. Chem.* **2019**, *58*, 8471. https://doi.org/10.1021/acs.inorgchem.9b00696
83. Häupler, B.; Schubert, U. S.; Wild, A.; Koutentis, P. A.; Zissimou, G. Ger. Offen. 10 2017 005924, 2018.
84. Steen, J. S.; Nuismer, J. L.; Eiva, V.; Wiglema, A. E. T.; Daub, N.; Hjelm, J.; Otten, E. *J. Am. Chem. Soc*. **2022**, *144*, 5051. https://doi.org/10.1021/jacs.1c13543
85. Saal, A.; Elbinger, L.; Schreyer, K.; Fataj, X.; Friebe, C.; Schubert, U. S. *ACS Appl. Energy Mater.* **2022**, *5*, 15019. https://doi.org/10.1021/acsaem.2c02559
86. Saal, A.; Friebe, C.; Schubert, U. S. *J. Power Sources* **2022**, *524*, 231061. https://doi.org/10.1016/j.jpowsour.2022.231061
87. Nicolaides, C.; Bazzi, F.; Vouros, E.; Flesariu, D. F.; Chrysochos, N.; Koutentis, P. A.; Constantinides, C. P.; Trypiniotis, T. *Nano Lett*. **2023**, *23*, 4579. https://doi.org/10.1021/acs.nanolett.3c01044
88. Poryvaev, A. S.; Gjuzi, E.; Polyukhov, D. M.; Hoffmann, F.; Fröba, M.; Fedin, M. V. *Angew. Chem. Int. Ed*. **2021**, *60*, 8683. https://doi.org/10.1002/anie.202015058
89. Peng, K.; Chen, H.; Shi, C.; Liu, S.; Hou, Y.; Yan, Y.; Li, Z.; Liu, S.; Zhang, L.; Hu, X.; Liu, X. *Mater. Horiz*. **2025**, *12*, 8667. https://doi.org/10.1039/D5MH00886G
90. Saenz, F.; Tamski, M.; Milani, J.; Roussel, C.; Frauenrath, H.; Ansermet, J.-P. *Chem. Commun*. **2022**, *58*, 689. https://doi.org/10.1039/D1CC05350G
91. Perras, F. A.; Flesariu, D. F.; Southern, S. A.; Nicolaides, C.; Bazak, J. D.; Washton, N. M.; Trypiniotis, T.; Constantinides, C. P.; Koutentis, P. A. *J. Phys. Chem. Lett.* **2022**, *13*, 4000. https://doi.org/10.1021/acs.jpclett.2c00748
92. Southern, S. A.; Zissimou, G. A.; Flesariu, D. F.; Bazzi, F.; Nicolaides, C.; Trypiniotis, T.; Constantinides, C. P.; Koutentis, P. A.; Perras, F. A. *J. Phys. Chem. Lett*. **2025**, *16*, 6219. https://doi.org/10.1021/acs.jpclett.5c01375
93. Constantinides, C. P.; Koutentis, P. A. In *Advances in Heterocyclic Chemistry*; Scriven, E. F. V.; Ramsden, C. A. Eds.; Academic Press: Amsterdam, 2016; Vol. 119, pp 173–207. https://doi.org/10.1016/bs.aihch.2016.03.001
94. Kumar, S.; Kumar, Y.; Keshri, S. K.; Mukhopadhyay, P. *Magnetochemistry* **2016**, *2*, 42. https://doi.org/10.3390/magnetochemistry2040042

95. Ji, Y.; Long, L.; Zheng, Y. *Mater. Chem. Front.* **2020**, *4*, 3433. https://doi.org/10.1039/d0qm00122h
96. Rogers, F. J. M.; Norcott, P. L.; Coote, M. L. *Org. Biomol. Chem.* **2020**, *18*, 8255. https://doi.org/10.1039/d0ob01394c
97. Gulyaev, D. A.; Gadimov, N. V.; Gritsan, N. P.; Kadilenko, E. M.; Shangin, P. G.; Syroeshkin, M. A.; Sosunov, E. A.; Tretyakov, E. V. *Mendeleev Commun*. **2025**, *35*, 169. https://doi.org/10.71267/mencom.7724
98. Gagné, R. R.; Koval, C. A.; Lisensky, G. C. *Inorg. Chem.* **1980**, *19*, 2854. https://doi.org/10.1021/ic50211a080
99. Bao, D.; Millare, B.; Xia, W.; Steyer, B. G.; Gerasimenko, A. A.; Ferreira, A.; Contreras, A.; Vullev, V. I. *J. Phys. Chem. A* **2009**, *113*, 1259. https://doi.org/10.1021/jp809105f
100. Dietrich, M.; Heinze, J. *J. Am. Chem. Soc.* **1990**, *112*, 5142. https://doi.org/10.1021/ja00169a023
101. Connelly, N. G.; Geiger, W. E. *Chem. Rev.* **1996**, *96*, 877. https://doi.org/10.1021/cr940053x
102. Pavlishchuk, V. V.; Addison, A. W. *Inorg. Chim. Acta*, **2000**, *298*, 97. https://doi.org/10.1016/S0020-1693(99)00407-7
103. Aranzaes, J. R.; Daniel, M.-C.; Astruc, D. *Can. J. Chem.* **2006**, *84*, 288. https://doi.org/10.1139/v05-262
104. Bird, M. J.; Iyoda, T.; Bonura, N.; Bakalis, J.; Ledbetter, A. J.; Miller, J. R. *J. Electroanal. Chem*. **2017**, *804*, 107. https://doi.org/10.1016/j.jelechem.2017.09.030
105. Miller, J. R.; Bird, M. J. In *Redox Chemistry – From Molecules to Energy Storage*. IntechOpen: London, 2022. https://doi.org/10.5772/intechopen.103003
106. Suryanarayanan, V.; Yoshihara, S.; Shirakashi, T. *Electrochim. Acta* **2005**, *51*, 991. https://doi.org/10.1016/j.electacta.2005.04.064
107. Elgrishi, N.; Rountree, K. J.; McCarthy, B. D.; Rountree, E. S.; Eisenhart, T. T.; Dempsey, J. L. *J. Chem. Educ*. **2018**, *95*, 197. https://doi.org/10.1021/acs.jchemed.7b00361
108. Pomikło, D.; Bodzioch, A.; Kaszyński, P. *J. Org. Chem*. **2023**, *88*, 2999. https://doi.org/10.1021/acs.joc.2c02703
109. Gulyaev, D. A.; Serykh, A.; Gurbunov, D.; Gritsan, N.; Akyeva, A.; Syroeshkin, M.; Romanenko, G.; Tretyakov, E. *Cryst. Growth Des*. **2024**, *24*, 5764. https://doi.org/10.1021/acs.cgd.4c00537
110. Chrysochos, N.; Constantinides, C. P.; Leitus, G. M.; Kourtellaris, A.; Lawson, D. B.; Deumal, M.; Ribas-Ariño, J.; Carvajal, M. À.; Zissimou, G. A.; Nicolaides, C.; Trypiniotis, T.; Koutentis, P. A. *Cryst. Growth Des.* **2023**, *23*, 8939. https://doi.org/10.1021/acs.cgd.3c00999
111. Bodzioch, A.; Pietrzak, A.; Kaszyński, P. *Org. Lett.* **2021**, *23*, 7508. https://doi.org/10.1021/acs.orglett.1c02733
112. Tang, W.; Steen, J. S.; Hettinga, J. W.; Hjelm, J.; Otten, E. *ACS Appl. Energy Mater.* **2025**, *8*, 18178.

https://doi.org/10.1021/acsaem.5c03070
113. Rajput, S. K.; Kaur, R.; Yadav, M.; Sahoo, A.; Chechik, V.; Samanta, P. K.; Mondal, P. C.; Mothika, V. S. *Small* **2026**, *22*, e10522. https://doi.org/10.1002/smll.202510522
114. Zhang, K.; Lin, X.; Shi, Y.; Oyaizu, K.; Jia, Z. *ACS Electrochem*. **2025**, *1*, 123. https://doi.org/10.1021/acselectrochem.4c00119
115. Kusamoto, T.; Kimura, S.; Ogino, Y.; Ohde, C.; Nishihara, H. *Chem. – Eur. J.* **2016**, *22*, 17725. https://doi.org/10.1002/chem.201602942
116. Ahmed, J.; Mandal, S. K. *Chem. Rev.* **2022**, *122*, 11369. https://doi.org/10.1021/acs.chemrev.1c00963
117. Hatakeyama-Sato, K.; Oyaizu, K. *Chem. Rev.* **2023**, *123*, 11336. https://doi.org/10.1021/acs.chemrev.3c00172
118. Kadassery, K. J.; Sethi, K.; Fanara, P. M.; Lacy, D. C. *Inorg*. *Chem*. **2019**, *58*, 4679. https://doi.org/10.1021/acs.inorgchem.9b00322
119. Gautam, R. K.; McGrath, J. J.; Wang, X.; Jiang, J. J. *J. Am. Chem. Soc*. **2024**, *146*, 28414. https://doi.org/10.1021/jacs.4c10106
120. Rawson, J. M.; Alberola, A.; Whalley, A. *J. Mater. Chem*. **2006**, *16*, 2560. https://doi.org/10.1039/b603199d
121. Gilroy, J. B.; McKinnon, S. D. J.; Koivisto, B. D.; Hicks, R. G. *Org. Lett.* **2007**, *9*, 4837. https://doi.org/10.1021/ol702163a
122. Steen, J. S.; de Vries, F.; Hjelm, J.; Otten, E. *ChemPhysChem* **2023**, *24*, e202200779. https://doi.org/10.1002/cphc.202200779
123. Kunz, S.; van Rensburg, M. J.; Pietruschka, D. S.; Achazi, A. J.; Emmel, D.; Kerner, F.; Mollenhauer, D.; Wegner, H. A.; Schröder, D. *Chem. Mater.* **2022**, *34*, 10424. https://doi.org/10.1021/acs.chemmater.2c02279

Authors' Biographies

Georgia A. Zissimou received her Ph.D. in Heterocyclic Chemistry from the University of Cyprus in 2019. She subsequently carried out postdoctoral research at the Centre of Molecular and Macromolecular Studies of the

Polish Academy of Sciences (Łódź, Poland) and later held an ONISILOS–Marie Skłodowska-Curie Actions Co-Fund Postdoctoral Fellowship. She is currently the principal investigator and coordinator of a Research and Innovation Foundation POST-DOC project at the University of Cyprus. Her research focuses on heterocyclic chemistry, stable organic radicals and zwitterions, molecular magnetism, electrochemistry, and functional organic materials, with particular emphasis on the design and synthesis of redox-active and spin-bearing molecular systems.